Patricia Wildberger

Aromatic interactions at the catalytic subsite of sucrose phosphorylase: Their roles in enzymatic glucosyl transfer probed with Phe52 → Ala and Phe52 → Asn muteins.

Diplomarbeit

zur Erlangung des akademischen Grades einer
Diplom-Ingenieurin
der Studienrichtung Biotechnologie
erreicht an der

Technischen Universität Graz

betreut durch:
Univ.-Prof. Dipl.-Ing. Dr. Bernd Nidetzky und
Dipl.-Ing. Dr. Christiane Gödl
Institut für Biotechnologie und Bioprozesstechnik

2010

Statutory Declaration

I declare that I have authored this thesis independently, that I have not used other than the declared sources/resources, and that I have explicitly marked all material which has been quoted either literally or by content from the used sources.

Date:

Signature:

Acknowledgement

I would like to thank my supervisor Univ.-Prof. Dipl.-Ing. Dr. Bernd Nidetzky for giving me the possibility to do my thesis in his group and for his excellent guidance and his constant feedback.

Thanks to Dipl.-Ing. Dr. Christiane Gödl, in particular, for patiently teaching me the concept of enzymology, for assisting me when I encountered questions during my workflow, for commenting and discussing the results I collected during the last months and for giving me excellent advice and support during the development of my thesis.

Very special thanks goes to the members of the Institute of Biotechnology and Biochemical Engineering for their constant support and the great working atmosphere. In particular I would like to thank my office colleagues with whom I spent a great time with fruitful discussions and enjoyable conversations.

My special appreciation goes to my boyfriend Jakob, my sister Katja and my parents as well as to my friends who kindly kept me grounded and always supported me with new motivation.

Kurzfassung

Interaktionen zwischen Proteinen und Kohlenhydraten spielen in biologisch relevanten Erkennungs- und Kommunikationsprozessen, wie zum Beispiel bei Immunreaktionen, Stoffwechselvorgängen, bakteriellen Infektionen sowie bei der Krebs-Metastase, eine wesentliche Rolle. Die Gegenwart von aromatischen Aminosäuren in der Bindetasche von Zucker verwertenden Enzymen hat sich als besonders wichtige Interaktion herausgestellt. Dabei stellt der aromatische Ring von Phenylalanin, Tryptophan oder Tyrosin eine geometrisch komplementäre apolare Oberfläche für Wechselwirkungen bereit und die π-Elektronenwolke interagiert mit den aliphatischen Protonen des Saccharides. Laut vorangegangenen in-silico Studien bekannter 3D-Strukturen besitzen Glykosidhydrolasen eine spezifische hydrophobe Plattform, bestehend aus einem (oder zwei) aromatischen Aminosäureresten. Solche aromatischen Interaktionen sind auch in der GH-13 Familie präsent, wo eine Interaktion zwischen einem Phenylalanin oder einem Tyrosin mit dem Glucosylring des Substrates konserviert ist. Saccharose Phosphorylase (SPase; EC 2.4.1.7) von *Leuconostoc mesenteroides* ist eine bakterielle Transglukosidase aus der GH 13 Familie, deren physiologische Funktion die reversible Umsetzung von Saccharose und Phosphat (P_i) in α-D-Glukose-1-Phosphat (G1P) und D-Fruktose darstellt. Mit Hilfe von zielgerichteter Mutagenese wurde in dieser Arbeit der aromatische Phenylalaninrest Phe52 der SPase von *L. mesenteroides* mit Alanine (F52A) und Asparagin (F52N) ersetzt und hinsichtlich der Auswirkungen auf den Reaktionsmechanismus untersucht. Detaillierte kinetische Studien zeigten, dass die katalytische Aktivität der beiden Mutanten, im Vergleich zum Wild-Typ Enzym, in Phosphorolyse-Richtung (Saccharose + $P_i \rightarrow$ G1P + Fruktose) signifikant verringert wurde und in Synthese-Richtung (G1P + Fruktose $\rightarrow$ Saccharose + P_i) komplett gehemmt wurde. Weiters konnte in dieser Arbeit gezeigt werden, dass der Phe52-Rest die Donorsubstrat-Spezifizität beeinflusst und für die strikte Präferenz des Wild-Typ Enzyms für Glukosylsubstrate mitverantwortlich ist. Im Wild-Typ Enzym steht der Phe52-Rest in sterischem Konflikt mit der axialen C-4 Hydroxygruppe von Galaktosylsubstraten und somit kann das Wild-Typ Enzym, im Gegensatz zu den Mutanten, keine Galaktosylsubstrate umsetzen.

Abstract

Interactions between proteins and carbohydrates play a significant role in biologically relevant recognition and communication processes, like in immune reactions, metabolism, bacterial infections and cancer metastasis. The presence of aromatic residues in the binding site of sugar-processing enzymes is found to be essential for protein-sugar interactions. The aromatic ring of phenylalanine, tryptophan or tyrosine provides a geometrically complementary apolar surface for interactions with the sugar ring and its π-electron cloud interacts with the aliphatic protons of the sugar that carry a positive charge. According to previous in-silico survey of known 3D-structures, glycoside hydrolases possess a family-specific hydrophobic platform consisting of one (or two) aromatic amino acid residues. Such an interaction can also be found in enzymes of the glycoside hydrolase family GH-13, where a phenylalanine or a tyrosine, stacking with the glucosyl ring of the substrate in the catalytic site, is strictly conserved. Sucrose phosphorylase (SPase; EC 2.4.1.7) from *Leuconostoc mesenteroides* is a bacterial transglucosidase that catalyzes the reversible conversion of sucrose and phosphate (P_i) into α-D-glucose-1-phosphate (G1P) and D-fructose. Using site-directed mutagenesis the Phe52 residue was replaced by alanine (F52A) and asparagine (F52N) and the effect of the mutation on the reaction mechanism of SPase was investigated. Detailed kinetic studies showed that the catalytic activity in phosphorolysis direction (sucrose + $P_i \rightarrow$ G1P + fructose) was significantly reduced in both muteins and activity in synthesis direction (G1P + fructose $\rightarrow$ sucrose + P_i) was completely disrupted. Additionally it could be shown that the Phe52 residue influences the substrate specificity and it seems from the structure of SPase that the presence of Phe52 generates a steric conflict with an axial hydroxyl at C-4 of galactosyl substrates, explaining the preference for glucosyl substrates in the wild-type enzyme and its loss in Phe52 muteins.

Contents

1 Aromatic interactions at the catalytic subsite of sucrose phosphorylase: Their roles in enzymatic glucosyl transfer probed with Phe52 → Ala and Phe52 → Asn muteins.

Patricia Wildberger, Christiane Luley-Goedl, Bernd Nidetzky*

Institute of Biotechnology and Biochemical Engineering, Graz University of Technology, Petersgasse 12/1, A-8010 Graz

1.1 Abstract

Replacement of Phe52 by Ala (F52A) and Asn (F52N) decreased the activity in phosphorolysis direction of *Leuconostoc mesenteroides* sucrose phosphorylase (*Lm*SPase) to about 0.34% (F52A) and 0.04% (F52N) of the wild-type level ($k_{cat} = 195\ s^{-1}$), whereas in synthesis direction, catalytic activity was completely disrupted in both muteins. The significant decrease in catalysis in phosphorolysis direction of the two mutants suggests that Phe52, through stacking interaction between the π-electron cloud of the aromatic residue and the aliphatic protons of the sugar, contributes to transition state stabilization. Disruption of catalysis in synthesis direction let assume that Phe52 has an important role on proper positioning of the leaving group. The 130,000-fold preference of the wild-type *Lm*SPase for glucosyl transfer from α-D-glucose-1-phosphate to arsenate compared with galactosyl transfer form α-D-galactose-1-phosphate to arsenate was changed to 21-fold and 6-fold for the F52A and F52N mutein, respectively. These results delineate the importance of Phe52 for substrate specificity. A steric conflict between the phenylalanine ring and the axial hydroxyl at C-4 of a galactosyl substrate could explain selectivity of the wild-type enzyme for glucosyl substrates and its preference loss in Phe52 muteins.

Keywords: Aromatic residue interaction; sucrose phosphorylase; glycoside hydrolase family GH-13; donor substrate selectivity

1.2 Introduction

Interactions between biomolecules and carbohydrates play a significant role in biologically relevant recognition processes including signal transduction, cell-cell interactions, pathogen entry to host cells, cancer metastasis, inflammation, fertility and development [1, 2, 3]. Apart from hydrogen bonding and solvation effects, the presence of aromatic residues in the binding site of sugar-processing enzymes is found to be indispensable for protein-sugar interactions [4, 5]. The protein-sugar interactions are characterized by the structure and conformation of the carbohydrate as well as the nature and orientation of the aromatic rings [4, 6] and have been considered as CH/π, van der Waals or hydrophobic interactions [7]. It is suggested that the aromatic ring provides a geometrically complementary apolar surface for interactions with the sugar ring and that its π-electron cloud interacts with the aliphatic protons of the sugar that carry a partial positive charge ($CH^{\delta+}$) [7, 8]. Tryptophan is often the preferred aromatic residue in the saccharide-binding site of proteins, although phenylalanine and tyrosine are also found. However, tryptophan, with its lager surface area, offers many more position-orientations for the saccharide to optimize its interactions with the other binding site residues [7]. Nerinckx et al. performed an in-silico survey of the -1 subsite of known 3D-structures of *O*-glycoside hydrolases and stated that all α- and β-*O*-pyranoside-glycoside hydrolases posses a family-specific hydrophobic platform consisting of one (or two) aromatic amino acid residues [9]. Such an interaction can also be found in enzymes of the glycoside hydrolase family GH 13, where a phenylalanine or a tyrosine, stacking with the glucosyl ring of the substrate in the catalytic site, is strictly conserved (Figure 1). Considering the crucial role of sugar-aromatic residue interactions for molecular recognition of carbohydrates in nature, it is surprising that the influence of those interactions on the catalytic mechanism of enzymes in family GH 13 has never been described before. Here we report for the first time on the investigation of an aromatic residue in the catalytic site of sucrose phosphorylase (SPase; EC 2.4.1.7) from *Leuconostoc mesenteroides* (*Lm*SPase). SPase is a bacterial transglucosidase that catalyzes the reversible conversion of sucrose (α-D-glucopyranosyl-1,2-β-D-fructofuranoside) and phosphate (P_i) into D-fructose and α-D-glucose-1-phosphate (G1P). The reaction

proceeds via a glycoside hydrolase-like double displacement mechanism that involves a catalytically competent β-glucosyl enzyme intermediate [10]. Using site-directed mutagenesis the Phe52 residue was replaced by alanine (F52A) and asparagine (F52N) to prevent interaction (a schematic picture of the stacking interaction is shown in Figure 2). Detailed kinetic studies of the resulting muteins were performed to determine the mutation-caused change of the catalytic efficiencies, the influence of aromatic stacking on transition-state stabilization and the change of donor substrate specificity.

A

Enzyme	Organism	GenBank	Sequence
Amylosucrase [11]	*Neisseria polysaccharea*	AAT15258.1	DGG**Y**^{154}AVS
Sucrose hydrolase [12]	*Xanthomonas axonopodis pv. glycines*	AAQ93678.1	DGG**F**^{139}AVS
α-Glucosidase [13]	*Geobacillus sp. HTA-462*	BAE48285.1	DNG**Y** ^{62}DIS
Isomaltulose synthase [14]	*Klebsiella sp. LX3*	AAK82938.1	DNG**Y**^{104}DIS
Cyclodextrin glycosyltransferase [15]	*Bacillus circulans*	CAA48401.1	YHG**Y**^{133}WAR
α-Amylase [16]	*Bacillus licheniformis*	AAA22226.1	YDL**Y** ^{90}DLG
Sucrose phosphorylase [17]	*Bifidobacterium adolescentis*	AAO33821.1	DAG**F** ^{53}DPI

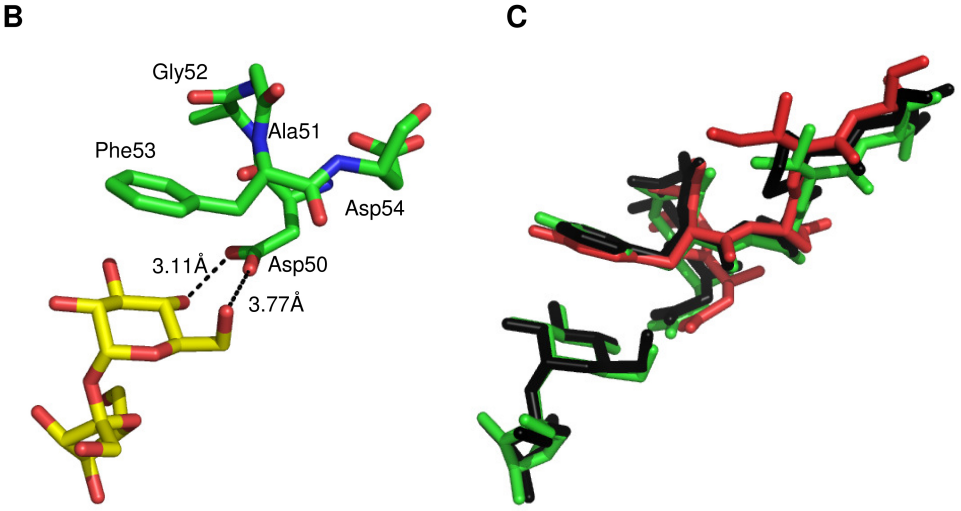

Figure 1: A) Comparison of aromatic-sugar interactions in the catalytic site of different GH-13 enzymes. Alignment was performed with the Clustal 2.0.12 multiple sequence alignment tool. Conserved aromatic residues are shaded in grey. B) Stacking interaction between the glucosyl ring of sucrose and the aromatic loop region in *Bifidobacterium adolescentis* SPase (2GDU) [18]. C) Overlay of SPase (2GDU; black), amylosucrase (1JGI; green) and isomaltulose synthase (1M53; red) aromatic loop regions. Average distance between the aromatic residue and the glucosyl ring was calculated to be 4.61 Å in SPase and 4.63 Å in amylosucrase.

1.3 Materials and methods

1.3.1 Site-directed mutagenesis and enzyme production

The point mutations Phe52 → Ala (F52A) and Phe52 → Asn (F52N) were introduced using a two-stage PCR protocol [19]. The pQE30 expression vector encoding the gene of wild-type *Lm*SPase was used as template [20]. One complementary pair of oligonucleotide primers was designed for each mutation (mismatched bases are underlined):

*Lm*SPase F52A forward: 5'-GGTGATCGCGGTGCTGCGCCAGC-3'
*Lm*SPase F52A backward: 5'-GCTGGCGCAGCACCGCGATCACC-3'
*Lm*SPase F52N forward: 5'-GGTGATCGCGGTAATGCGCCAGC-3'
*Lm*SPase F52N backward: 5'-GCTGGCGCATTACCGCGATCACC-3'

In the first step, two separate PCR reactions with the forward and backward primer were performed which consisted of a preheating step at 95°C for 60 s followed by 4 reaction cycles (95°C, 50 s/60°C, 50 s/72°C, 10 min). In the second step, PCR reactions were combined and continued for 18 reaction cycles (95°C, 50 s/60°C, 50 s/72°C, 10 min). The amplification product was subjected to parental template digest by *Dpn*I and transformed into electro-competent *E. coli* Top10 cells. Mini-prep plasmid DNA was sequenced in order to verify the introduction of the desired substitutions. The *Lm*SPase wild-type and muteins encoding genes were digested from the pQE30 vector using Fast Digest restriction enzymes *Bam*HI and *Pst*I (Promega). Ligation into the dephosphorylated pASK-IBA7+ expression vector was done using a T4-DNA ligase (Promega). Strep-tagged wild-type and muteins encoding genes were sequenced in sense and antisense directions.
E. coli Top10 cells, transformed with the corresponding pASK-IBA7+ expression plasmid, were cultivated in 1-L baffeled shaken flasks at 37°C and 110 rpm using LB-media and 115 mg/L ampicillin. When OD_{550} reached 0.5-0.6, temperature was decreased to 25°C and gene expression was induced with 200 μg/L anhydrotetracycline for 6 h. Cells were harvested by centrifugation at 4°C and 5,000 rpm for 30 min in a Sorvall RC-5B Refrig-

erated Superspeed centrifuge. Resuspended cells were frozen at -20°C, thawed and the suspension was passed twice through a French pressure cell press (Aminco). Cell debris was removed by centrifugation at 4°C, 14,000 rpm for 45 min. The resulting supernatant was used for further purification of *Lm*SPase-F52A and *Lm*SPase-F52N.

1.3.2 Purification and characterization

All purification steps were carried out at 6°C on a Duoflow system (BioRad). The elution of proteins was monitored at 280 nm. All buffer solutions were degassed and filtered using 0.2 μm cellulose-acetate and 0.2 μm Sartolon polyamide filters (Sartorius). The crude cell extract was passed through an 1.2 μm cellulose-acetate filter (Sartorius) before loading on a Strep-Tactin Superflow column (binding capacity 100 nmol/mL; bed volume 5 mL). Note that Strep-tagged *Lm*SPase has a molecular weight of 59 kDa, which results in a loading capacity of 30 mg. For a detailed description of the purification procedure see Supplementary Information.

1.3.3 Enzyme assays

Enzyme activity in the direction of sucrose phosphorolysis was determined at 30°C using a continuous coupled enzymatic assay with phosphoglucomutase and glucose-6-phosphate dehydrogenase as described elsewhere [20]. Protein concentrations were determined using the BioRad dye-binding method with BSA as standard. Glucose was determined using a coupled enzymatic assay with hexokinase and glucose-6-phosphate dehydrogenase [21]. Glucose in the presence of fructose was determined using a coupled enzymatic assay with glucose oxidase and peroxidase [22]. Galactose was assayed using a galactose dehydrogenase based assay (galactose dehydrogenase (0.6 U/mL), 2.2 mM NAD^+ in 90 mM Tris/HCl, pH 8.6) where the formation of NADH with time was monitored spectrophotometrically at 340 nm. G1P was assayed in a coupled enzymatic system with phosphoglucomutase and glucose-6-phosphate dehydrogenase [23]. Phosphate was deter-

mined colorimetrically at 850 nm [24].

1.3.4 Kinetic studies

Initial-rate measurements of glucosyl transfer to and from phosphate were carried out at 30°C in 50 mM MES buffer, pH 7.0 using discontinuous assays, in which formation of G1P and phosphate was determined, respectively. The concentration of one substrate was kept constant at saturating concentrations of 5-10 times its apparent K_m value, while the other substrate was varied. Each assay contained approximately 0.3 mg/ml of *Lm*SPase-F52A or *Lm*SPase-F52N. Control reactions lacking the enzyme or one of the substrates were performed in all cases and values reported are corrected for those readings. Substrate concentrations were varied in the range of 10 μM to 3 mM for G1P, 1 mM to 850 mM fructose, 1 mM to 100 mM for phosphate and 5 mM to 800 mM for sucrose. Kinetic parameters were obtained from non-linear fits of the data to equation 1:

$$\nu = k_{cat} \cdot E \cdot \frac{S}{K_m + S} \tag{1}$$

where ν is the observed reaction rate [mM/min], k_{cat} is the catalytic constant [min^{-1}], E is the total molar enzyme concentration based on a molecular mass of 59 kDa for the protein subunit [mM], S is the substrate concentration [mM] and K_m is the apparent Michaelis-constant [mM]. Instead of phosphate, arsenate can be used as alternative glycosyl acceptor substrate. In contrast to the reversible reaction of phosphorolysis, arsenolysis is irreversible. Using G1P or galactose-1-phosphate (Gal1P) as donor substrate, the obtained α-glycopyranosyl arsenate product decomposes hydrolytically [25] yielding glucose or galactose, arsenate and phosphate, respectively. The rate of arsenolysis was determined at 30°C in 50 mM MES buffer, pH 7.0 using discontinuous assays [50 mM arsenate, 50 mM G1P or 50 mM Gal1P, in the presence of 0.15 mg/mL enzyme], in which formation of glucose or galactose was measured. Hydrolytic activity of the wild-type *Lm*SPase and muteins towards G1P and sucrose was determined at 30°C in 50 mM MES buffer, pH 7.0 using discontinuous assays [20 mM G1P, enzyme concentration 0.2 mg/mL (muteins)

and 0.02 mg/mL *Lm*SPase wild-type; 500 mM sucrose, enzyme concentration 0.2 mg/mL for *Lm*SPase wild-type and muteins respectively] under conditions in which a suitable nucleophile (phosphate or fructose) was lacking.

1.4 Results and discussion

1.4.1 Influence of the F52A and F52N mutation on the reaction mechanism of *Lm*SPase.

In a new approach of producing recombinant *Lm*SPase, the affinity tag was changed. The enzyme carries an 8 amino acid long N-terminal fused Strep-Tactin affinity tag, instead of an 11 amino acid long N-terminal fused His-tag [20]. The specific enzyme activities were not affected by the different tags and the purification procedure was simplified by using a two step protocol for the Strep-tagged enzyme, compared to a three step protocol for the His-tagged enzyme [25]. A detailed kinetic characterization of the F52A and F52N mutein showed that all enzyme activities were significantly decreased. Depicted in Scheme 1 is the proposed reaction mechanism for the SPase catalyzed phosphorolysis and synthesis of sucrose. The catalytic activity in phosphorolysis direction was decreased to about 0.34% (F52A) and 0.04% (F52N) of the wild-type level as shown in Table 1. The K_m for sucrose increased indefinitely and also the catalytic efficiency for sucrose was significantly lower as compared to the wild-type (18 and 87 times for F52A and F52N, respectively). The K_m for phosphate was only moderately changed, but $[k_{cat}/K_m]_{Pi}$ decreased drastically (139-fold and 6,833-fold for F52A and F52N, respectively). These results indicate that the absence of the stacking interaction between the glucosyl ring of sucrose and the aromatic residue lead to a weak binding of sucrose and consequently to a decrease in the catalytic efficiency for the formation of the covalently linked glucosyl-enzyme intermediate ($[k_{cat}/K_m]_{Suc}$). Moreover, the drastic decrease in the catalytic efficiency for the deglucosylation step $[k_{cat}/K_m]_{Pi}$ let assume that a major contribution to transition stabilization is missing due to the replacement of the aromatic residue.

The decrease in k_{cat}/K_m can be expressed as loss of transition state stabilization energy, using Equation 2, where $\Delta\Delta G$ is the free energy change [kcal/mol], $[k_{cat}/K_m]_{mut}$ is the

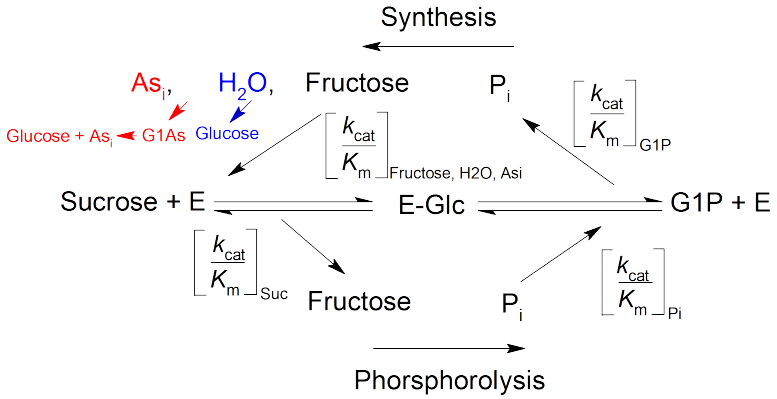

Scheme 1: Reaction mechanism of SPase proceeds in two catalytic steps via a covalent glucosyl-enzyme intermediate (E-Glc). Enzymatic reaction in phosphorolysis direction (lower panel) and synthesis direction (upper panel) is shown. The E-Glc can react with phosphate (phosphorolysis), fructose (synthesis), H_2O (hydrolysis) or with an alternative glucosyl acceptor substrate like arsenate (As_i, arsenolysis).

catalytic efficiency associated with the muteins, $[k_{cat}/K_m]_{wt}$ is the catalytic efficiency associated with the wild-type, R is the gas constant [8.31 J mol^{-1} K^{-1}] and T is the temperature [303.15 K].

$$\Delta\Delta G = -RT \cdot ln([k_{cat}/K_m]_{mut}/[k_{cat}/K_m]_{wt}) \tag{2}$$

According to Spiwok et al., interaction energies of a pyranose moiety with a side chain of an aromatic residue were calculated as attractive with interaction energies ranging from -2.8 to -12.3 kcal/mol. The most attractive interaction was associated with an apparent combination of CH/π interactions and classical H-bonds [27]. The important role of aromatic amino acid residues in the catalytic site of carbohydrate-active enzymes and the significant decrease in activity or affinity for substrates upon mutation of the aromatic residues were studied in various proteins [28, 29] but never in an enzyme from family GH13. We could show that the replacement of the aromatic residue Phe52 by alanine and asparagine in *Lm*SPase led to a significant drop in activity and substrate affinity. Summarized in Table 1 are the results from the calculated free energy changes. According to $\Delta\Delta$G values, the catalytic efficiency for the deglucosylation step ($[k_{cat}/K_m]_{Pi}$) was more significantly affected than the catalytic efficiency for the glucosylation step ($[k_{cat}/K_m]_{Suc}$)

Table 1: Kinetic parameters in phosphorolysis direction and apparent k_{cat} values for the arsenolysis and hydrolysis reactions catalyzed by wild-type *Lm*SPase and muteins.

Reaction type		Wild-type	F52A mutant	F52N mutant
k_{cat} [s^{-1}]		165	n.a.	n.a.
K_m [mM]	Phosphorolysis	5.70	n.a.	n.a.
[k_{cat}/K_m] [s^{-1} mM^{-1}]	50 mM P_i 5 mM – 800 mM Sucrose	28.7	1.64	0.33
ΔΔG [kcal/mol]		-	1.7	2.7
k_{cat} [s^{-1}]		195[a]	0.66	0.08
K_m [mM]	Phosphorolysis 500 mM Sucrose	9.50[a]	4.45	25.8
[k_{cat}/K_m] [s^{-1} mM^{-1}]	1 mM – 100 mM P_i	20.5[a]	0.148	0.003
ΔΔG [kcal/mol]		-	3.0	5.3
k_{cat} [s^{-1}]	G1P Arsenolysis	49.4	0.04	0.02
k_{cat} [s^{-1}]	Gal1P Arsenolysis (10^{-4})	3.80	19.0	35.0
k_{cat} [s^{-1}]		1.60	0.01	0.03
K_m [mM]	G1P Hydrolysis	17.2	0.38	0.63
[k_{cat}/K_m] [s^{-1} mM^{-1}]	20 mM G1P	0.09	0.04	0.03
ΔΔG [kcal/mol]		-	0.57	0.60

[a]250 mM sucrose was used [26]; n.a., not applicable

although the binding affinity of sucrose was indefinitely increased. A plausible explanation could be that due to the missing interaction between the glucosyl moiety and the aromatic residue the stabilization of the transition state is drastically weakened.

1.4.2 Disruption of the enzymatic activity in synthesis direction.

To encore with the significantly lower activity in phosphorolysis direction, the catalytic activity in synthesis direction was completely disrupted in both muteins. Varying fructose concentrations in the presence of a saturating concentration of G1P did not alter the catalytic reaction rate, revealing a non-effective binding of fructose (see Supplementary Figure 3). On the contrary, G1P showed a very high binding affinity towards the

*Lm*SPase muteins (K_m = 0.38 mM for F52A; K_m = 0.63 mM for F52N). These findings in combination with the absence of any product accumulation within the detection limit of the performed NMR analysis led to the assumption that sugar transfer from the glucosyl-enzyme intermediate to fructose was disrupted due to an irreconcilable distance between the donor and the acceptor. Instead of product formation, hydrolysis occurred. Interestingly, the hydrolytic activity (k_{cat}) towards G1P was 160 times (F52A) and 53 times (F52N) lower as compared to the wild-type (see Table 1). The free energy change $\Delta\Delta$G for $[k_{cat}/K_m]_{G1P}$ was calculated to be 0.57 and 0.60 kcal/mol for F52A and F52N, respectively and revealed only a moderate change although k_{cat} and K_m values were significantly affected. Reactions catalyzed by the *Lm*SPase wild-type proceed in a two-step double displacement-like mechanism via the formation of a covalent intermediate. Any assumption about an alternative reaction mechanism used by the muteins was disproved by arsenolysis experiments because arsenate can only react when the glucosyl-enzyme intermediate has been formed (see Scheme 1) [25].

1.4.3 Change of donor substrate selectivity.

When Mueller et al. [30] was investigating the role of Asp-295 in the molecular mechanism of *Lm*SPase, the replacement by asparagine and glutamate reduced the selectivity for glucosyl and promoted the one for mannosyl donors. Wild-type *Lm*SPase is highly specific for transferring glucosyl residues. We compared activity of *Lm*SPase in synthesis reactions that used G1P or Gal1P as donor substrate. On the molecular level, the aromatic residue and the axial hydroxyl at C-4 of a galactosyl donor substrate would cause a steric conflict. According to our expectations, arsenolytic activity towards Gal1P was slightly increased to about 5.0- and 9.2-fold of the wild-type level ($k_{cat} = 3.8 \cdot 10^{-4}$ s^{-1}) when Phe52 was replaced by alanine and asparagine, respectively. Arsenolysis of G1P was still detectable with both muteins however it was 1,235 (F52A) and 2,470 (F52N) lower compared to the wild-type (k_{cat} = 49.4 s^{-1}). Thus, the donor substrate selectivity (G1P/Gal1P) was changed from 130,000 for the wild-type enzyme, to 21 and 6 for the F52A and F52N

mutein, respectively. This indicates that the large preference of the *Lm*SPase wild-type for the arsenolysis reaction with G1P was nearly completely lost in both muteins. SPase is a suitable biocatalyst in the production of industrial fine chemicals [31], therefore it is of concern to enhance the donor substrate selectivity. Thus, an engineered SPase which is capable of transferring galactosyl moieties to various acceptor substrates is of high interest.

1.5 Conclusions

The important role of aromatic stacking interactions at the catalytic subsite is revealed by the required pre-arranged complementarity between the aliphatic protons of the sugar moiety and the aromatic residue, which is present in all glycoside hydrolases. According to the sequence based classification of glycoside hydrolases and glycosyltransferases, SPase is a glycoside hydrolase [32], more precisely a transglucosidase, which shows the typical aromatic stacking interactions in the catalytic subsite. Upon mutation of the Phe52 residue the transition state stabilization was significantly affected. Thus, the binding affinity of sucrose decreased significantly which can be explained by the missing electrostatic interactions between the aliphatic protons of the donor substrate in the ground-state $^4C_1$ conformation and the π-electron cloud of the aromatic residue. The dramatic change in catalytic activities of glucosyl transfer, which is expected to proceed through an oxocarbenium ion-like transition state [33], can be explained by the lacking stabilization of the Phe52 residue on the sugar ring, which is constrained to a $^4H_3$ half-chair transition state conformation. Furthermore, the aromatic residue has an effect on the relative positioning of the nucleophile, depicted by the complete disruption of the catalytic activity in synthesis direction. Phe52 is further involved in discrimination between glucosyl and galactosyl donors. Although the catalytic turnover number is drastically reduced compared to the wild-type, this is a useful approach to investigate donor substrate selectivity and to generate SPase muteins with a different glycosyl donor spectrum.

1.6 References

[1] Bucior, I. and Burger M. (2004). Carbohydrate-carbohydrate interactions in cell recognition. Curr. Opin. Struct. Biol., 631-637.

[2] Nangia-Makker P., Conklin J., Hogan V., and Raz A. (2002). Carbohydrate-binding proteins in cancer, and their ligands as therapeutic agents. Trends. Mol. Med., 187-192.

[3] Ratner D.M., Adams E.W., Disney M.D., and Seeberger P.H. (2004). Tools for glycomics: Mapping interactions of carbohydrates in biological systems. ChemBioChem, 1375-1383.

[4] Diaz M.D., Fernandez-Alonso M.D., Cueves G., Canada F.J., and Jimenez-Barbero J. (2008). On the role of aromatic-sugar interactions in the molecular recognition of carbohydrates: A 3D view by using NMR. Pure Appl. Chem., 1827-1835.

[5] Quiocho F.A. (1989). Protein-carbohydrate interactions: Basic molecular features. Pure Appl. Chem., 1293-1306.

[6] Sujatha M.S., Sasidhar Y.U., and Balaji P.V. (2007). MP2/6-311++G(d,p) study on galactose-aromatic residue analog complexes in different position-orientations of the saccharide relative to aromatic residue. J. Mol. Struct, 11-24.

[7] Sujatha M.S., Sasidhar Y.U., and Balaji P.V. (2004). Energetics of galactose- and glucose-aromatic amino acid interactions: Implications for binding in galactose-specific proteins. Protein Sci., 2502-2514.

[8] Sujatha M.S., Sasidhar Y.U., and Balaji P.V. (2005). Insights into the role of the aromatic residue in galactose-binding sites: MP2/6-311G++** study on galactose- and glucose-aromatic residue analogue complexes. Biochemistry, 8554-8562.

[9] Nerinckx W., Desmet T., and Claeyssens M. (2003). A hydrophobic platform as a mechanistically relevant transition state stabilising factor appears to be present in the active centre of all glycoside hydrolases. FEBS Lett., 1-7.

[10] Goedl C., Schwarz A., Mueller M., Brecker L., and Nidetzky B. (2008). Mechanistic differences among retaining disaccharide phosphorylases: Insights from kinetic analysis of active site mutants of sucrose phosphorylase and α,α-trehalose phosphorylase. Carbohydr. Res., 2032-2040.

[11] Mirza O., Skov L.K., Remaud-Simeon M., Potocki de Montalk G., Albenne C., Monsan P., and Gajhede M. (2001). Crystal structures of amylosucrase from *Neisseria polysaccharea* in complex with D-glucose and the active site mutant Glu328Gln in complex with the natural substrate sucrose. Biochemistry, 9032-9039.

[12] Kim M., Kim H.S., Jung J., and Rhee S. (2008). Crystal structures and mutagenesis of sucrose hydrolase from *Xanthomonas axonopodis pv. glycines*: Insight into the exclusively hydrolytic amylosucrase fold. J. Mol. Biol., 636-647.

[13] Shirai T., Hung V.S., Morinaka K., Kobayashi T., and Ito S. (2008). Crystal structure of GH13 α-glucosidase GSJ from one of the deepest sea bacteria. Proteins, 126-133.

[14] Zhang D., Li N., Lok S.M., Zhang L.H., and Swaminathan K. (2003). Isomaltulose synthase (*Pal*I) of *Klebsiella sp. LX3*. Crystal structure and implication of mechanism. J. Biol. Chem., 35428-35434.

[15] Klein C. and Schulz G. E. (1991). Structure of cyclodextrin glycosyltransferase refined at 2.0 Å resolution. J. Mol. Biol., 737-750.

[16] Machius M. , Wiegand G. , and Huber R. (1995). Crystal structure of calcium-depleted *Bacillus licheniformis* α-amylase at 2.2 Å resolution. J. Mol. Biol., 545-559.

[17] Mirza O., Skov L.K., Sprogøe D., van den Broek L.A.M., Beldman G., Kastrup J.S., and Gajhede M. (2006). Structural rearrangements of sucrose phosphorylase from *Bifidobacterium adolescentis* during sucrose conversion. J. Biol. Chem., 35576-35584.

[18] Sprogøe D., van den Broek L.A.M., Mirza O., Kastrup J.S., Voragen G.J., Gajhede M., and Skov L.K. (2004). Crystal structure of sucrose phosphorylase from *Bifidobacterium adolescentis*. Biochemistry, 1156-1162.

[19] Wang W. and Malcolm B. A. (1999). Two-stage PCR protocol allowing introduction of multiple mutations, deletions and insertions using QuikChange Site-Directed Mutagenesis. Biotechniques, 680-682.

[20] Goedl C., Schwarz A., Minani A., and Nidetzky B. (2007). Recombinant sucrose phosphorylase from *Leuconostoc mesenteroides*: Characterization, kinetic studies of transglucosylation, and application of immobilised enzyme for production of α-D-glucose 1-phosphate. J. Biotechnol., 77-86.

[21] Kunst A., Draeger B., and Ziegenhorn J. (1984). UV-methods with hexokinase and glucose-6-phosphate dehydrogenase. Verlag Chemie, 163-172.

[22] Kunst A., Draeger B., and Ziegenhorn J. (1984). D-glucose. Colorimetric methods with glucose oxidase and peroxidase. Verlag Chemie, 178-185.

[23] Michal G. (1984). D-glucose 1-phosphate. Verlag Chemie, 185-191.

[24] Saheki S., Takeda A., and Shimazu T. (1985). Assay of inorganic phosphate in the mild pH range, suitable for measurement of glycogen phosphorylase activity. Anal. Biochem., 277-281.

[25] Schwarz A. and Nidetzky B. (2006). Asp-196 $\rightarrow$ Ala mutant of *Leuconostoc mesenteroides* sucrose phosphorylase exhibits altered stereochemical course and kinetic mechanism of glucosyl transfer to and from phosphate. FEBS Lett., 3905-3910.

[26] Schwarz A., Brecker L., and Nidetzky B. (2007). Acid-base catalysis in *Leuconostoc mesenteroides* sucrose phosphorylase probed by site-directed mutagenesis and detailed kinetic comparison of wild-type and Glu237 $\rightarrow$ Gln mutant enzymes. Biochem. J., 441-449.

[27] Spiwok V., Lipovová P., Skálová T., Vondrácková E., Dohnálek J., Hasek J., and Králová B. (2005). Modelling of carbohydrate-aromatic interactions: *ab initio* energetics and force field performance. J. Comput.-Aided Mol. Des., 887-901.

[28] Huber R.E., Hakda S., Cheng C., Cupples C.G., and Edwards R.A. (2003). Trp-999 of β-galactosidase (*Escherichia coli*) is a key residue for binding, catalysis, and synthesis of allolactose, the natural *Lac* operon inducer. Biochemistry, 1796-1803.

[29] Muraki M., Harata K., Sugita N., and Sato K. I. (2000). Protein-carbohydrate interactions in human lysozyme probed by combining site-directed mutagenesis and affinity labeling. Biochemistry, 292-299.

[30] Mueller M. and Nidetzky B. (2007). The role of Asp-295 in the catalytic mechanism of *Leuconostoc mesenteroides* sucrose phosphorylase probed with site-directed mutagenesis. FEBS Lett., 1403-1408.

[31] Goedl C., Sawangwan T., Mueller M., Schwarz A., and Nidetzky B. (2008). A high-yielding biocatalytic process for the production of 2-*O*-(α-D-glucopyranosyl)-*sn*-glycerol, a natural osmolyte and useful moisturizing ingredient. Angew. Chem. Int. Ed., 10086-10089.

[32] Goedl C., Sawangwan T., Wildberger P., and Nidetzky B. (2010). Sucrose phosphorylase: A powerful transglucosylation catalyst for synthesis of glucosides as industrial fine chemicals. Biocat. and Biotrans., 10-21.

[33] Goedl C. and Nidetzky B. (2009). Sucrose phosphorylase harbouring a redesigned, glycosyltransferase-like active site exhibits retaining glucosyl transfer in the absence of a covalent intermediate. ChemBioChem, 2333-2337.

1.7 Supplementary information

1.7.1 NMR spectroscopy.

Reaction mixtures contained *Lm*SPase-F52A or *Lm*SPase-F52N (0.6 mg/mL), 20 mM G1P and 100 mM fructose in 50 mM MES buffer (pH 7.0) and were incubated at 30°C for 120 h.

The reaction mixtures were lyophilized, dissolved in D2O (99.95%, 0.7 mL) and used for NMR spectroscopic data recording without further purification. Samples were transferred into 5 mm high precision NMR sample tubes (Promochem, Wesel, Germany). All spectra were recorded on a Bruker DRX-400 AVANCE spectrometer (Bruker, Rheinstetten, Germany) at 300K and 400.13 MHz (^{1}H), 100.61 MHz (^{13}C) or 161.98 MHz (^{31}P) using the Bruker Topspin 1.3 software. For 1D-spectra, 32k data points were acquired using a relaxation delay of 1.0 s and an appropriate number of scans for reasonable signal to noise ratios. After zero filling to 64k data points and Fourier transformation, spectra with a range of 7,200 Hz (^{1}H), 20,000 Hz (^{13}C) and 16,200 Hz (^{31}P) were obtained, respectively. To determine the 2D COSY, TOCSY, NOESY, HMQC, and HMBC as well as ^{1}H/^{31}P-HMQC spectra, 128 experiments with 8 scans and 1024 data points each were performed. After linear forward prediction to 256 data points in the f_2-dimension and appropriate sinusoidal multiplication in both dimensions, the data were Fourier transformed in order to obtain 2D-spectra with ranges of 4,000 Hz (^{1}H), 20,000 Hz (^{13}C) and 8,100 Hz (^{31}P). Chemical proton and carbon shifts were referenced to external acetone (^{1}H: δ_H 2.225 ppm; ^{13}C: δ_C 31.45 ppm) and phosphorus shifts were referenced to external aqeous 85% phosphoric acid (^{31}P: δ_P 0.00 ppm).

1.7.2 Enzyme purification.

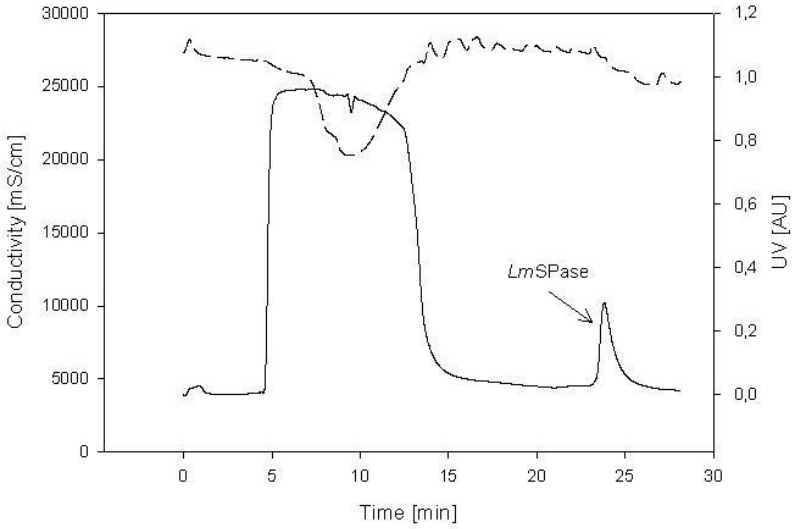

Supplementary Figure 1: Typical chromatogram recorded during purification of the *Lm*SPase-F52N mutant by Strep-Tactin affinity chromatography. The column was equilibrated with buffer W (100 mM Tris/HCl, 150 mM NaCl, 1 mM EDTA, pH 8.0) at a flow rate of 3 mL/min (5 column volumes). The crude cell extract was applied (2.5-12.5 min) at a flow rate of 1 mL/min. After washing with buffer W (12.5-20.5 min) at a flow rate of 2 mL/min (5 column volumes), the *Lm*SPase containing fractions were eluted (20.5-28 min) with buffer E (100 mM Tris/HCl, 150 mM NaCl, 1 mM EDTA, 2.5 mM desthiobiotin, pH 8.0) at a flow rate of 2 mL/min (3 column volumes).

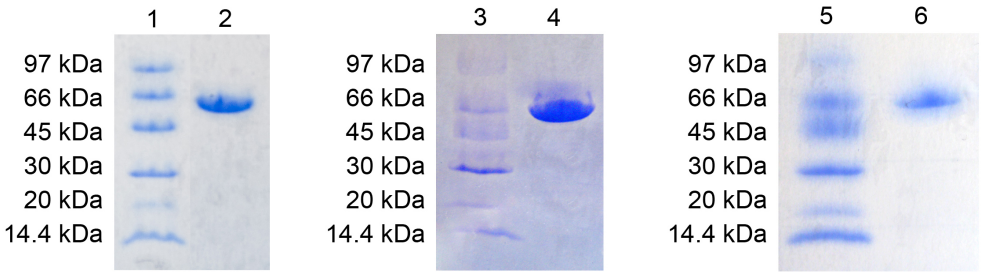

Supplementary Figure 2: Purification monitored by SDS-PAGE. Precast gradient gels (PhastGel 8-25) were used on a PhastSystem from GE Healthcare. Lane 1,3,5: LMW-standard; 2: purified enzyme fraction LmSPase-F52N; 4: purified enzyme fraction wild-type; 6: purified enzyme fraction LmSPase-F52A.

1.7.3 Kinetic studies

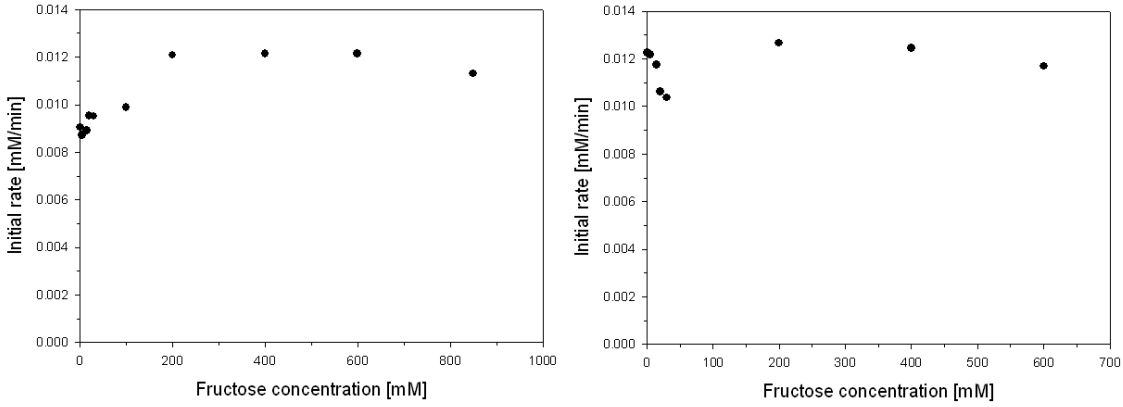

Supplementary Figure 3: Michaelis-Menten plots for the determination of kinetic parameters in synthesis direction catalyzed by LmSPase-F52A (left plot) and LmSPase-F52N (right plot). Initial-rates were determined as function of Pi release using a discontinuous assay. The enzymatic assay was performed in 50 mM MES buffer, pH 7.0 at 30°C and 550 rpm at saturating concentrations of 20 mM G1P.

2 Sucrose phosphorylase: a powerful transglucosylation catalyst for synthesis of α-D-glucosides as industrial fine chemicals

Biocatalysis and Biotransformation, January–February 2010; 28(1): 10–21

informa
healthcare

ORIGINAL ARTICLE

Sucrose phosphorylase: a powerful transglucosylation catalyst for synthesis of α-D-glucosides as industrial fine chemicals

CHRISTIANE GOEDL, THORNTHAN SAWANGWAN, PATRICIA WILDBERGER, & BERND NIDETZKY

Institute of Biotechnology and Biochemical Engineering, Graz University of Technology, Graz, Austria

Abstract
Sucrose phosphorylase is a bacterial transglucosidase that catalyzes conversion of sucrose and phosphate into α-D-glucose-1-phosphate and D-fructose. The enzyme utilizes a glycoside hydrolase-like double displacement mechanism that involves a catalytically competent β-glucosyl enzyme intermediate. In addition to reaction with phosphate, glucosylated sucrose phosphorylase can undergo hydrolysis to yield α-D-glucose or it can decompose via glucosyl transfer to a hydroxy group in suitable acceptor molecules, giving new α-D-glucosidic products. The glucosyl acceptor specificity of sucrose phosphorylase is reviewed, focusing on applications of the enzyme in glucoside synthesis. Polyhydroxylated compounds such as sugars and sugar alcohols are often glucosylated efficiently. Aryl alcohols and different carboxylic acids also serve as acceptors for enzymatic transglucosylation. The natural osmolyte 2-*O*-(α-D-glucopyranosyl)-*sn*-glycerol (GG) was prepared by regioselective glucosylation of glycerol from sucrose using the phosphorylase from *Leuconostoc mesenteroides*. An industrial process for production of GG as active ingredient of cosmetic formulations has been recently developed. General advantages of sucrose phosphorylase as a transglucosylation catalyst lie in the use of sucrose as a high-energy glucosyl donor and the usually weak hydrolase activity of the enzyme towards substrate and product.

Keywords: *Disaccharide phosphorylase, transglucosylation, acceptor specificity, sucrose, glucosylglycerol*

Introduction

Sucrose phosphorylase (sucrose:phosphate α-D-glucosyltransferase; EC 2.4.1.7) catalyzes the reversible conversion of sucrose (α-D-glucopyranosyl-1,2-β-D-fructofuranoside) and phosphate into α-D-glucopyranosyl phosphate (Glc1P) and D-fructose. The KEGG database indicates involvement of the enzyme in breakdown as well as synthesis of sucrose. However, the equilibrium constant of the phosphorylase reaction at pH 7.0 and 30°C was determined as 44 (Goedl et al. 2007), and the physiological concentration of phosphate is expected to be larger than that of Glc1P. Therefore, sucrose phosphorylase is likely to serve a catabolic function *in vivo*, fueling the energy metabolism of the cell with Glc1P (and D-fructose) produced from sucrose.

The enzyme has been characterized from a relatively small number of bacterial species, namely *Bifidobacterium adolescentis* (van den Broek et al. 2004), *Leuconostoc mesenteroides* (Koga et al. 1991; Kawasaki et al. 1996; Lee et al. 2006; Goedl et al. 2007), *Pseudomonas saccharophila* (Weimberg & Doudoroff 1954; Silverstein et al. 1967; Tsai et al. 1980) and *Streptococcus mutans* (Robeson et al. 1983; Ferretti et al. 1988; Russell et al. 1988). Genes encoding putative sucrose phosphorylases have been detected mainly in members of the bacterial class of *Bacillus* spp. The enzyme is about 500 amino acids long and was found to occur as a functional monomer or dimer (Table I). Its activity is not dependent on cofactors or cosubstrates. In the sequence-based categorization of glycoside hydrolases and glycosyltransferases (Cantarel et al. 2009), sucrose phosphorylase is a member of family GH13, also widely known as the α-amylase family (Janecek et al. 1997). Therefore, despite its EC classification as glucosyltransferase, the phosphorylase is structurally most related to enzymes of the glycoside hydrolase class (EC 3.2). A similar 'dichotomy' in categorization based on sequence and function exists for other

Correspondence: B. Nidetzky, Institute of Biotechnology and Biochemical Engineering, Graz University of Technology, Petersgasse 12/1, A-8010 Graz, Austria. Tel: +43-316-873-8400. Fax: +43-316-873-8434. E-mail: bernd.nidetzky@tugraz.at

ISSN 1024-2422 print/ISSN 1029-2446 online
DOI: 10.3109/10242420903411595

Table I. Comparison of sucrose phosphorylases from different sources.

Microorganism	Native molecular mass (kDa) (gel filtration)	Molecular mass (kDa) (SDS-PAGE)	pH optimum[a] (phosphorolysis)	Functional oligomeric state	Reference
B adolescentis	129.0	58.0	6.0–6.5, 48°C	dimeric	van den Broek et al. (2004)
L. mesenteroides	56.4	56.4		monomeric	Koga et al. (1991)
	58.0– 60.0	54.0–58.0	7.0–7.5, 30°C		Kawasaki et al. (1996)
		56.0	6.2–6.5, 37°C		Lee et al. (2006)
		55.3	6.7, 37°C		Lee et al. (2008)
		60.0	6.5–7.0, 30°C		Goedl et al. (2007)
P. saccharophila			6.6–6.8, 30°C		Weimberg & Doudoroff (1954)
	84.0		7.0, 30°C		Silverstein et al. (1967)
	78.0	50.0		dimeric	Tsai et al. (1980)
					Vandamme et al. (1987)
S. mutans		55.0	6.5, 37°C	monomeric	Robeson et al. (1983)
	55.7				Ferretti et al. (1988)
					Russell et al. (1988)

[a]The pH optimum was determined at indicated temperatures.

disaccharide phosphorylases (maltose and trehalose phosphorylases – GH65; cellobiose and chitobiose phosphorylases – GH94; lacto-*N*-biose phosphorylase – GH112). Stam et al. (2006) have recently subclassified family GH13 based on enzyme functional properties. Sucrose phosphorylases form subfamily 18. A crystal structure has been determined for the homodimeric sucrose phosphorylase from *B. adolescentis* (Sprogoe et al. 2004). The enzyme adopts the canonical $(\beta/\alpha)_8$-barrel fold of glycoside hydrolases and transglycosidases of family GH13 (Figure 1A). The active-site residues, a triad of two aspartic acids and one glutamic acid, are highly conserved in both sequence and structure (Figure 1B).

Biochemical studies of sucrose phosphorylase go back in time to the 1940s. The enzyme was discovered first in *L. mesenteroides* (Kagan et al. 1942) and *P. saccharophila* (Doudoroff 1943). Mieyal & Abeles (1972) summarize evidence from early mechanistic work on sucrose phosphorylase that led to the perceptive proposal of a double displacement-like reaction mechanism involving a catalytically competent covalent enzyme intermediate. A β-configured *O*-glycosidic linkage between the glucosyl moiety and a carboxylate side chain from Asp/Glu was demonstrated (Voet & Abeles 1970). The proposed covalent intermediate has now also been seen crystallographically (Mirza et al. 2006). Residues involved in catalysis were probed and their proposed function confirmed by kinetic characterization of relevant site-directed mutants (Schwarz & Nidetzky 2006; Mueller & Nidetzky 2007; Schwarz et al. 2007). Asp^{192} (amino acid numbering of *B. adolescentis*) is the catalytic nucleophile, Glu^{232} is the catalytic

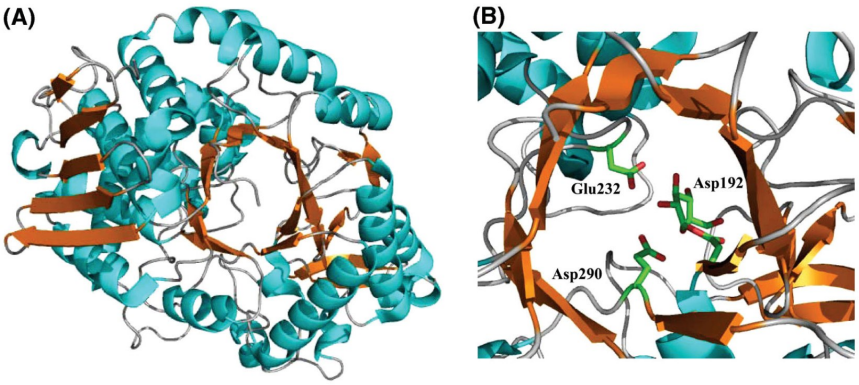

Figure 1. (A) Three-dimensional fold for the subunit of sucrose phosphorylase from *B. adolescentis* derived from the crystal structure of the dimeric enzyme (PDB entry 1r7a). (B) Close-up structure of the active site in the β-glucosyl enzyme intermediate of the phosphorylase (PDB entry 2gdv, chain a). Residues of the catalytic triad, Asp^{192} (nucleophile; glucosylated in the structure), Glu^{232} (acid–base) and Asp^{290} (transition state stabilizer), are indicated.

acid–base, and Asp^{290} functions as a transition state stabilizer. By forming a strong hydrogen bond with the hydroxyl groups at C2 and C3 of the glucosyl residue being transferred, the anionic side chain of Asp^{290} is suggested to provide selective stabilization to oxocarbenium ion-like transition states flanking the covalent (α)-glucosyl enzyme intermediate. The proposed two-step catalytic mechanism of sucrose phosphorylase is summarized in Scheme 1.

Sucrose phosphorylase is known to catalyze three types of overall reaction, as shown in Scheme 2: glucosyl transfer to and from phosphate, often termed *phosphorolysis* and *synthesis*; hydrolysis; and transglucosylation. Arsenate can replace phosphate as glucosyl acceptor substrate. However, because α-glucopyranosyl arsenate decomposes hydrolytically in a non-enzymatic reaction, the overall arsenolysis of sucrose is essentially irreversible. Hydrolysis and transglucosylation are reactions of the glucosylated phosphorylase under conditions when phosphate (or arsenate) is lacking. Hydrolysis occurs at a rate ≥50 times more slowly than glucosyl transfer to phosphate. External acceptors differ in reactivity towards glucosylation by the phosphorylase, as discussed later.

Sucrose, Glc1P and α-glucopyranosyl fluoride (Glc1F) are highly reactive donor substrates for the enzyme. Some authors have used nitrophenyl-α-D-glucopyranose as substrate to assay the activity of sucrose phosphorylase. However, using the enzyme from *L. mesenteroides*, we find that nitrophenyl-α-D-glucopyranose is converted in phosphorolysis about 1000 times more slowly than sucrose (Wiesbauer et al. unpublished results). Alternative (very) slow substrates of the enzyme – e.g. α-D-mannopyranosyl phosphate (Mueller & Nidetzky 2007) and α-D-glucopyranosyl azide (Schwarz et al. 2007) – are not considered here. The range of acceptor substrates is broad (for earlier reviews, see Mieyal & Abeles 1972; Vandamme et al. 1987), defining the scope for sucrose phosphorylase as a useful transglucosylation catalyst. The crystallographically observed conformational flexibility of the acceptor-binding site in sucrose phosphorylase (from *B. adolescentis*) may be key to the accommodation of a diverse group of compounds to become glucosylated. The purpose of this review is to put previous studies on transglucosylation by sucrose phosphorylase into a coherent whole. Focus is on preparative application of phosphorylase-catalyzed synthesis of α-D-glucosides.

Transglycosylation

Sucrose phosphorylase catalyzes glucosyl transfer with retention of the α-anomeric configuration of the donor substrate in the resulting glucosidic product. The enzyme shares its double displacement-like catalytic mechanism (Scheme 1) with the vast majority of glycoside hydrolases and transglycosidases that catalyze their reactions via configurational, α→α or β→β retention (Lairson & Withers 2004). Interception of the glycosyl enzyme intermediate by external acceptors is the common mechanistic basis for transglycosylation by these enzymes (Crout & Vic 1998). Transfer to acceptor usually occurs under strong competition with reaction of water. The transglycosylation product is by definition a substrate of the enzyme and can therefore be degraded by secondary hydrolysis. An 'ideal' biocatalytic system for transglycosylation would efficiently prevent *primary hydrolysis* of the glycosylated enzyme and also show low reactivity towards the glycosyl transfer product (*secondary hydrolysis*). Both primary and secondary hydrolysis decrease the atom economy of the biotransformation. Furthermore, the hydrolysis product may inhibit the enzyme and it can serve as an unwanted glycosyl acceptor, leading to contamination of the glycosidic product derived from the transglycosylation process.

The glycosyl donor substrate should be a chemically stable and benign ('green') compound. However, its reactivity towards the enzyme should be sufficient to provide a high steady-state concentration of the covalent intermediate. Thermodynami-

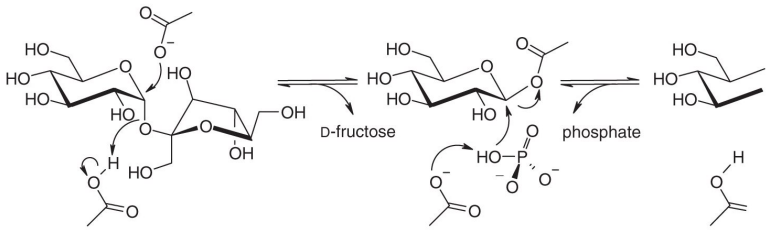

Scheme 1. Proposed catalytic mechanism for sucrose phosphorylase. The enzymatic reaction proceeds in two catalytic steps via a covalent enzyme intermediate. For reasons of clarity, only the catalytic nucleophile (top) and the general acid–base (bottom) are shown.

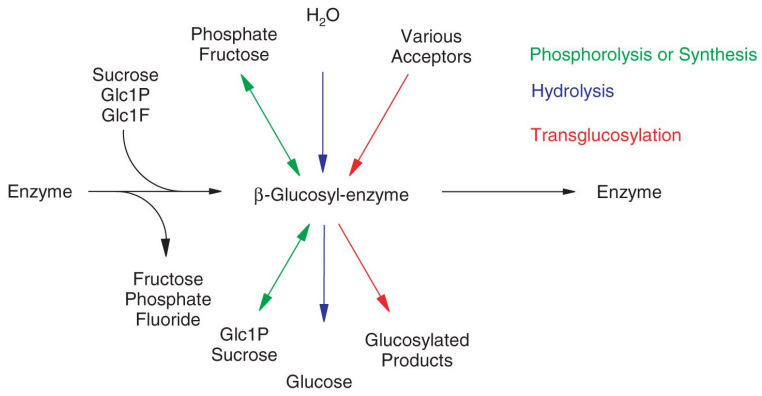

Scheme 2. Three types of overall reactions catalyzed by sucrose phosphorylases. The β-glucosyl enzyme intermediate can react with phosphate (phosphorolysis) and fructose (synthesis) shown in green, with water (hydrolysis) shown in blue, or with various other acceptors (transglucosylation) shown in red. Double arrows indicate reversible reactions.

cally, the donor substrate should drive the overall transglycosylation towards product. We show that the system sucrose phosphorylase and sucrose differs from other transglycosylation catalysts in that it fulfils these requirements very well. The following discussion of synthetic applications of sucrose phosphorylase first considers the role of the donor substrate and focuses then on the different acceptor structures derivatized by the enzyme.

Role of the donor substrate

In terms of catalytic efficiency (k_{cat}/K_M measured at a saturating concentration of phosphate), sucrose is a 5.4-fold better donor substrate for glucosylation of sucrose phosphorylase (from *L. mesenteroides*) than is Glc1P (Schwarz et al. 2007). Glc1F would be a similarly efficient substrate as sucrose (Mieyal & Abeles 1972; Goedl & Nidetzky 2009). Considering the equilibrium constant for phosphorolysis of sucrose (Goedl et al. 2007), the overall thermodynamic driving force for glucosylation to proceed from sucrose will be substantially higher than that for the same transformation starting from Glc1P. Kinetic studies in which sucrose and Glc1P were compared as substrates for glucosylation of glycerol reveal that the covalent intermediate of *L. mesenteroides* sucrose phosphorylase reacted more efficiently with the acceptor when sucrose instead of Glc1P was employed as glucosyl donor (Goedl et al. 2008a). Enhanced transglucosylation efficiency could result from a truly increased reactivity of the glucosylated enzyme towards glycerol when sucrose is present or it could be apparent and reflect (partial) suppression of the reaction with water under these conditions. Whatever explanation is correct, in practical terms however, sucrose is the clearly preferred choice of donor substrate for the enzyme.

Polyhydroxylated acceptors

A number of sugars and sugar alcohols have been glucosylated, with variable efficiency, by sucrose phosphorylase. The resulting saccharides and glucosyl polyols could be useful as food additives and cosmetic ingredients. There is currently considerable interest in non-digestible (oligo)saccharides acting as prebiotics (Gibson & Roberfroid 1995). Sugar alcohols and their glycosylated derivatives are potential inhibitors of dental plaque formation and can serve as alternative sweeteners (Havukkala 1991). Furthermore, inhibitory activity of glucosylated oligosaccharides on α-amylase and α-glucosidase suggests medical applications such as in blood sugar regulation (Yoon & Robyt 2003).

Aggregate data from the literature reveal that glucosylation of polyhydroxylated acceptors occurs with relatively high regioselectivity. A *cis* diol group appears to be preferentially recognized by the enzyme (Doudoroff et al. 1947). However, the acceptor motif is not essential for glucosyl transfer to occur because primary alcohols (methanol, ethanol, trans-1,2-cyclohexanediol) also function as slow substrates of the enzyme (Vandamme et al. 1987). Using sugar alcohols, the secondary hydroxyl of the terminal diol moiety becomes glucosylated (Kitao & Sekine 1992). A detailed structure–activity relationship analysis for glucosyl transfer to polyhydroxylated acceptors is not possible using the available data on enzyme specificity which are usually not quantitative. The typical categorization of acceptors used in literature is good – intermediate – poor. However, a

molecular basis for recognition of sucrose by the phosphorylase from *B. adolescentis* is now available from the crystallographic studies of Mirza et al. (2006). Although slight differences in polyhydroxylated acceptor substrate utilization may exist among sucrose phosphorylases from different organisms, the overall pattern of specificity is conserved (Doudoroff et al. 1947; Kitao & Sekine 1992; van den Broek et al. 2004; Lee et al. 2006).

Glycerol, xylitol, D- as well as L-arabitol, and D-sorbitol are glucosylated with good efficiency. L-Sorbose, D-xylulose, L-ribulose and D-rhamnulose are also good acceptor substrates. With the exception of L-arabinose, aldose sugars are poorly used. However, synthesis of α-D-glucopyranosyl-1,1-β-D-arabinofuranoside was achieved using glucosylation of D-arabinose by *B. adolescentis* sucrose phosphorylase (van den Broek et al. 2004). Keto-aldoses such as 2-keto-L-arabinose (Doudoroff et al. 1947) and 2-keto-D-xylose (Hassid et al. 1946) yielded transfer products. α-Methyl-D-glucose was unreactive (van den Broek et al. 2004). Disaccharides and higher oligosaccharides featuring α- or β-type glycosidic linkage were generally not transformed by phosphorylases from different sources. The enzyme from *L. mesenteroide*s B-1149 was an exception because it gave a transfer efficiency >10% (from TLC analysis) to lactose, cellobiose, maltotriose and isomaltotriose (Lee et al. 2006). However, the resulting products were not identified. Table II summarizes results of glucosylation studies in which the transfer product was isolated and characterized structurally. Details of the synthesis procedure are also given in the table. Scheme 3 displays the structures of the studied polyhydroxylated glucosyl acceptors. Use of glycerol as acceptor substrate is discussed in a separate section later.

Some authors (Kitao & Sekine 1992; van den Broek et al. 2004) noted that in glucosylation processes using Glc1P as donor substrate, a number of acceptors (e.g. xylitol) showed much higher (apparent) activity than D-fructose. Considering the relatively unfavorable equilibrium constant for synthesis of sucrose, these observations may contain a thermodynamic effect and are perhaps not explicable solely on differences in enzymatic reactivity. Equilibrium constants for synthesis of glucosyl transfer products from Glc1P or sucrose are generally not available. However, synthesis of sucrose may be thermodynamically more demanding than, for example, synthesis of glucosyl xylitol.

In contrast to D-fructose for which glucosylation by sucrose phosphorylase seems to yield only a single transfer product (sucrose), reaction of *L. mesenteroides* phosphorylase with D-glucose gave a mixture of regioisomeric disaccharides, namely kojibiose

Table II. Glucosylation of selected polyhydroxy acceptors using purified, recombinant sucrose phosphorylase from (A) *B. adolescentis*; (B) *L. mesenteroides* and (C) partially purified sucrose phosphorylase from dry *P. saccharophila* cells. Structure elucidation of the transglucosylation product was performed by XRD and NMR analysis.

	Donor (w/v)	Acceptor (w/v)	Optimized reaction conditions	Transglucosylation product	Mass of isolated product	Reference
A	Glc1P, 25%	D-Arabinose, 15%	pH 6.5, 30°C, 10 U mL^{-1}	α-D-Glucopyranosyl-β-D-arabinofuranose	n.d.	van den Broek et al. (2004)
B	Glc1P, 30%	Xylitol, 30%	pH 6.9, 42°C, 45 U mL^{-1}	4-*O*-(α-D-Glucopyranosyl)-xylitol	3.0 g, 100 mL	Kitao & Sekine (1992)
	Sucrose, 20%	D-Glucose, 20%	pH 6.9, 42°C, 30 U mL^{-1}	2-*O*-(α-D-Glucopyranosyl)-α-D-glucopyranose 3-*O*-(α-D-Glucopyranosyl)-α-D-glucopyranose	n.d.	Kitao et al. (1994)
	Sucrose, 27%	Glycerol, 18%	pH 7.0, 30°C, 20 U mL^{-1}	2-*O*-(α-D-Glucopyranosyl)-*sn*-glycerol	10.2 g, 90 mL	Goedl et al. (2008a)
	Sucrose, 10%	*R*-Glycerate, 3%	pH 7.0, 30°C, 20 U mL^{-1}	*R*-2-*O*-(α-D-Glucopyranosyl)-glycerate	3.3 g, 110 mL	Sawangwan et al. (2009)
C	Glc1P, 5%	L-Sorbose, 3.7%	pH 7.4, 37°C, 5 g[a]	α-D-Glucopyranosyl-α-L-sorbofuranose	0.4 g, 300 mL	Hassid et al. (1945)
	Glc1P, 6%	D-Ketoxylose, 2%	pH 7.4, 37°C, 7.5 g[a]	α-D-Glucopyranosyl-β-D-ketoxylofuranose	0.3 g, 680 mL	Hassid et al. (1946)
	Glc1P, 6%	L-Ketoarabinose, 2%	pH 7.4, 37°C, 7.5 g[a]	α-D-Glucopyranosyl-β-L-ketoarabinofuranose	0.8 g, 680 mL	Doudoroff et al. (1947)
	Glc1P, 7.5%	L-Arabinose, 4%	pH 7.0, 35°C, 5 g[a]	3-*O*-(α-D-Glucopyranosyl)-L-arabinopyranose	5.4 g, 400 mL	Hassid et al. (1948)
	Sucrose, 5%	D-Rhamnulose, 0.5%	pH 7.4, 30°C, n.d.	α-D-Glucopyranosl-β-D-rhamnulofuranose	0.2 g, 50 mL	Palleroni & Doudoroff (1956)

Glc1P, α-D-glucopyranosyl phosphate; n.d., not documented.
[a]Mass of dry bacteria cells used for enzyme preparation.

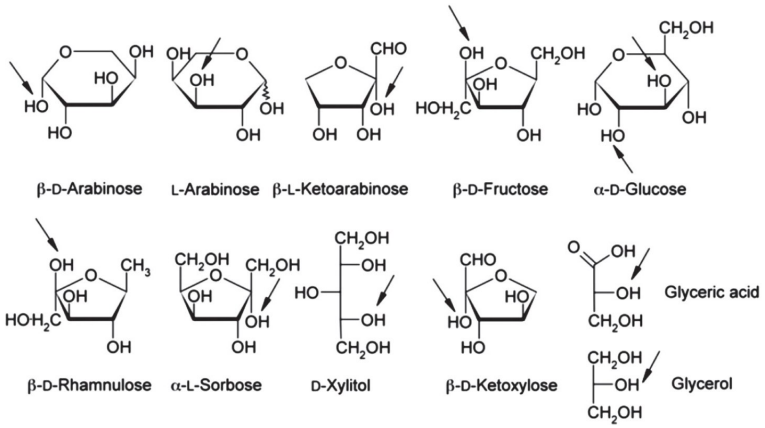

Scheme 3. Glucosyl acceptors having a polyhydroxylated structure. Glucosylation sites are indicated by an arrow.

(α-D-glucopyranosyl-1,2-D-glucose) and nigerose (α-D-glucopyranosyl-1,3-D-glucose) in a mass ratio of about 2:1 (Kitao et al. 1994). Formation of these 'glucobiose' products in high amounts was observed when enzyme was incubated with sucrose and D-glucose. Use of a substrate mixture of Glc1P and D-glucose gave ~6-fold lowered yield. Interestingly, incubation of *L. mesenteroides* sucrose phosphorylase in the presence of sucrose, however in the absence of external D-glucose, also yielded kojibiose and nigerose in amounts exceeding by a factor of ~2 those obtained from Glc1P and D-glucose. Therefore, these results imply that the possibility of glucosylation of D-glucose should be considered in transglucosylation processes where a substantial amount of D-glucose is formed as result of donor substrate hydrolysis. They furthermore support the notion that glucosyl transfer to acceptor is generally favored under conditions when sucrose rather than Glc1P is used as glucosyl donor.

Recent applications of sucrose phosphorylase-catalyzed glucosylations include chemo- and regioselective synthesis of *R*-2-*O*-α-D-glucopyranosyl-glycerate (Sawangwan et al. 2009), a bacterial compatible solute that has potential applications as a protein stabilizer (Empadinhas & da Costa 2008, Sawangwan et al. 2010), and formation of a nucleotide sugar, α-D-glucopyranosyl cytosine monophosphate (Lee et al. 2008). Glucosylation of cytosine monophosphate occurred at a phosphate hydroxy group. Analogs of natural nucleotide sugars are of interest in the development of drugs for the clinical treatment of human cancers or viral diseases (Zhihua et al. 2009). Interestingly, despite its high selectivity for glucosylation of the 2-OH in glycerate, sucrose phosphorylase from *L. mesenteroides* showed only little discrimination between the *R* and *S* antipodes of this acceptor so that *S*-2-*O*-α-D-glucopyranosyl-glycerate could likewise be produced with the enzyme (Sawangwan et al. 2009).

Acceptors containing phenolic, benzylic and other hydroxy groups

Glycosylation at phenolic or benzylic hydroxy groups is a well-known strategy exploited by nature to enhance the bioavailability of poorly soluble aromatic compounds. Glycosylation is also suggested to augment the stability of (poly)phenols to oxidative degradation (Kitao et al. 1993). It can improve compatibility of the product with the desired application which in the case of complex aromatic structures may be related to food, medicine and healthcare, and cosmetic formulations. Sucrose phosphorylase was used successfully to glucosylate a number of acceptors containing hydroxy groups attached to aromatic and unsaturated ring structures, some of which are shown in Scheme 4. The solubility of acceptor substrates and inactivation of the enzyme in the presence of acceptor are, however, issues requiring attention. Reactions were usually performed in the presence of a very large (≥50-fold) molar excess of donor over acceptor substrate. The given yields are typically based on acceptor converted (Table III).

Glucosylation of phenolic hydroxy groups by the enzyme from *L. mesenteroides* was strongly dependent on the nature and position of substituents on the aromatic ring (Kitao & Sekine 1994a). In a series of benzene diols and triols, hydroxy groups in *ortho* and *para* position favored transformation as compared with reaction of phenol. A hydroxymethyl substituent on the aromatic ring was in itself hardly reactive; a carboxylic acid substituent was inactive. The presence of both substituents generally decreased the

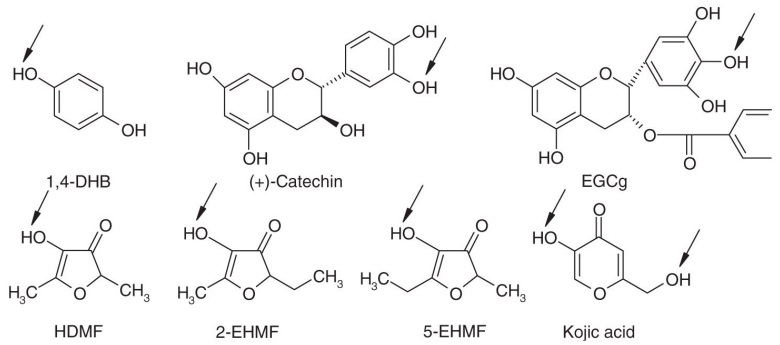

Scheme 4. Structures of glucosyl acceptors containing hydroxy groups attached to aromatic and unsaturated ring structures. Glucosylation sites are indicated by an arrow.

reactivity of the phenolic hydroxyl as compared with the analogous hydroxyl in the corresponding benzenediol acceptor. Glucosylation of catechol (benzene-1,2-diol), resorcinol (benzene-1,3-diol) and hydroquinone (benzene-1,4-diol) was examined in more detail. The transfer product of the reaction with hydroquinone was isolated and characterized structurally as well as functionally (Table III). Glucosylation strongly stabilized the hydroquinone moiety against oxidation induced by light irradiation. In a recent study, Wiesbauer et al. (unpublished results) showed that hydrolysis of donor substrate during glucosylation of 2,6-difluorophenol by phosphorylase from *L. mesenteroides* can be prevented when using a mutated enzyme in which the acid–base catalyst Glu^{237} was replaced by the incompetent Gln. However, the downsides of the Glu^{237}→Gln mutated phosphorylase are its relatively low activity (≤1% of wild-type level) and that sucrose cannot be used as donor substrate.

Successful transformation of various polyphenols was also reported (Kitao et al. 1993). Products resulting from the conversion of (+)-catechin and (–)-epigallocatechin gallate were characterized structurally (Table III) and some functional properties (solubility, resistance to oxidative decomposition, antioxidant activity) were determined. The apparently high selectivity of *L. mesenteroides* sucrose phosphorylase for reaction with the 3′-hydroxy group of (+)-catechin (Scheme 4) is remarkable. With (–)-epigallocatechin gallate (Kitao et al. 1995), two transfer products were obtained (Table III). Polyphenols have a multitude of biological effects considered beneficial, including antimutagenic and antibacterial activities. Glucosylated versions of these compounds are thus expected to be suitable fine chemicals for use in foods, cosmetic products and drugs.

Another group of bioactive compounds that could benefit from glucosylation are the hydroxyfuranones, with 4-hydroxy-2,5-dimethyl-3(2*H*)-furanone (HDMF), 2-ethyl-4-hydroxy-5-methyl-3(2*H*)-furanone (2-EHMF) and 5-ethyl-4-hydroxy-2-methyl-3(2*H*)-furanone (5-EHMF) being prominent representatives. HDMF is a flavor component of fruits and heat-processed foods. EHMFs are major aroma components in Japanese-style soy sauce and are likewise found in fermented soybean paste. HDMF and EHMFs are effective anticarcinogens and possess antioxidative properties against lipid peroxidation (Koga et al. 1998). However, HDMF and EHMFs are unstable and volatile. In addition to providing a stabilizing effect, glucosylation results in a change in physical properties as compared with the free furanones. HDMF has a fruity odor, similar to pineapple, whereas the glucosylated counterpart is odorless. EHMFs are obtained as pale yellow syrups of caramel-like appearance and have an intense sweet odor. The glucosylated products are white and odorless powders. Using sucrose phosphorylase from *L. mesenteroides*, Kitao et al. (2000) prepared glucosyl derivatives of HDMF and EHMFs in reasonable yields (Table III). The antioxidative activity of the furanone glucosides was weak. However, it was proposed that the compounds might be employed as pro-active ingredients.

Glucosylation of kojic acid (Kitao & Sekine 1994b) and vitamin C (Kwon et al. 2007) are yet other interesting applications of sucrose phosphorylase in synthesis. Both molecules are of broad interest for their antioxidative properties. Glucosyl derivatives could be more stable than the parent compounds. Kojic acid was reactive in a transglucosylation catalyzed by sucrose phosphorylase from *L. mesenteroides* (Table III) whereas vitamin C was not (Kitao & Sekine 1992). Both the phenolic hydroxy group and the hydroxymethyl group of kojic acid were derivatized. A doubly modified kojic acid was, however, not reported. Vitamin C was glucosylated using the enzyme from *Bifidobacterium longum* and 2-*O*-α-D-glucopyranosyl-L-ascorbic acid was obtained

Table III. Glucosylation of phenolic acceptors using sucrose phosphorylase from *L. mesenteroides*. Transfer yields were calculated based on the limiting substrate concentration. Structure elucidation of the transglucosylation product was performed by secondary-ion MS and NMR analysis.

Sucrose (w/v)	Acceptor (w/v)	Optimized reaction conditions	Transfer yield	Transglucosylation product	Mass of isolated product[a]	Reference
50%	1,4-DHB, 1%	pH 7.5, 37°C, 50 U mL^{-1}	82%	Hydroquinone 1′-*O*-α-D-glucopyranose	2.3 g, 100 mL	Kitao & Sekine (1994a)
30%	(+)-Catechin, 1%	pH 7.5, 42°C, 50 U mL^{-1}[b]	81%	(+)-Catechin 3′-*O* α-D-glucopyranose	0.2 g, 100 mL	Kitao et al. (1993)
30%	EGCg, 1%	pH 6.0, 42°C, 50 U mL^{-1}[b]	70%	EGCg 4′-*O*-α-D-glucopyranose EGCg 4′,4″-*O*-α-D-diglucopyranose	0.3 g, 100 mL 0.5 g, 100 mL	Kitao et al. (1995)
50%	HDMF, 5%	pH 7.2, 32°C, 500 U mL^{-1}	45%	HDMF 4-*O*-α-D-glucopyranose	0.8 g, 100 mL	Kitao et al. (2000)
50%	EHMFs, 5%	pH 7.2, 32°C, 500 U mL^{-1}	48%	2-EMF 4-*O*-α-D-glucopyranose 5-EMF 4-*O*-α-D-glucopyranose	0.9 g, 100 mL	
40%	Kojic acid, 2%	pH 7.5, 42°C, 90 U mL^{-1}[c]	20%	Kojic acid 5-*O*-α-D-glucopyranose Kojic acid 7-*O*-α-D-glucopyranose	0.3 g, 100 mL 0.4 g, 100 mL	Kitao & Sekine (1994b)

1,4-DHB, benzene-1,4-diol (hydroquinone); EGCg, epigallocatechin gallate; HDMF, 4-hydroxy-2,5-dimethyl-3(2*H*)-furanone; EHMF, 2-ethyl-4-hydroxy-5-methyl-3(2*H*)-furanone or 5-ethyl-4-hydroxy-2-methyl-3(2*H*)-furanone; kojic acid, 5-hydroxy-2-(hydroxymethyl)-4-pyrone.
[a]Preparative synthesis differed from optimized reaction conditions. [b]2% (v/v) methanol. [c]20% (v/v) dimethylsulfoxide in the reaction mixture.

(Kwon et al. 2007). Like in the case of catechin glucosides, the resulting product is pro-active and antioxidative properties of vitamin C are reinstalled upon hydrolysis. In contrast to synthesis by sucrose phosphorylase, previous strategies of glucosylation of vitamin C gave product mixtures (Muto et al. 1990; Aga et al. 1991).

Transfer to carboxylic groups

Sugimoto et al. (2007) reported on a novel reaction catalyzed by sucrose phosphorylase (from *S. mutans*) in which a carboxylic group becomes glucosylated at low pH. The enzyme from *L. mesenteroides* was also active in the same reaction, however, much less so than the streptococcal phosphorylase. Figure 2 compares pH profiles of the activity of sucrose phosphorylase catalyzing glucosyl transfer from sucrose to phosphate, hydroquinone and acetic acid. The optimum pH of 6.5 seen for enzymatic glucosylation of phosphate and hydroquinone was shifted to pH 5.0 when acetic acid was used as glucosyl acceptor. The protonated form of the carboxylic group may be required for reaction to take place (Sugimoto et al. 2007). Superior stability of the enzyme from *S. mutans* at low pH, as compared with *L. mesenteroides* enzyme, probably explains the difference in efficiency between the two phosphorylases (Sugimoto et al. 2007). Short-chain fatty acids, hydroxy acids, dicarboxylic acids and aromatics were identified as potential glucosyl acceptors, the corresponding transfer ratios being in the range 10–90% (based on acceptor converted). Glucosylation of benzoic acid (Sugimoto et al. 2007) and acetic acid (Nomura et al. 2008) was examined in more detail (Table IV). These biotransformations are of interest because certain industrial applications of carboxylic group-containing compounds (Scheppach et al. 1992; Kim & Won 1998) are limited by the strong sour smell and taste of the compound. Another problem can be a too low solubility.

The primary transglucosylation product was always 1-*O*-acyl α-D-glucopyranose. This underwent intramolecular acyl migration and mutarotation to yield 2-*O*-acyl α-D-glucopyranose and 2-*O*-acyl β-D-glucopyranose, respectively, as seen in earlier chemical work on 1-*O*-acyl β-D-glucopyranuronates (Fenselau 1994). Because acyl migration is strongly dependent on pH, the composition of the product mixture obtained by phosphorylase-catalyzed glucosylation of carboxylic substrates varied in dependence of the reaction conditions (Sugimoto et al. 2007). High sucrose concentrations in the range of 40% (w/v) were required for good transfer yield (~80%). Interestingly, the threshold value of the sour taste for acetyl glucopyranose was approximately 100 times increased compared with acetic acid.

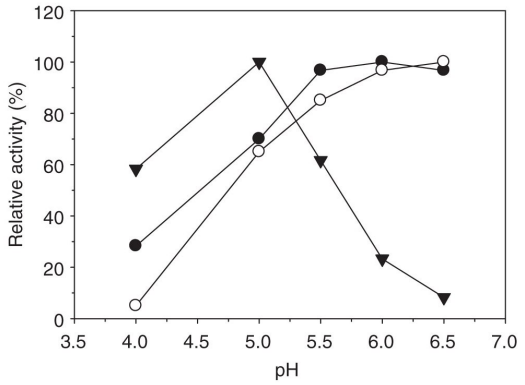

Figure 2. Effect of pH on phosphorolysis of sucrose (●) and glucosyl transfer from sucrose to hydroquinone (○) or acetic acid (▲) catalyzed by sucrose phosphorylase from *S. mutans*. Reaction mixtures contained: for phosphorolysis, enzyme (3 U mL^{-1}), sucrose (5% w/v) and phosphate (0.1 M); for transglucosylation, enzyme (60 U mL^{-1}), sucrose (40% w/v) and hydroquinone (1.2% w/v) or acetic acid (1.2% w/v) dissolved in the appropriate buffer. Incubation was carried out at 37°C for 30 min. Data are related to highest activity as 100%.

However, a slightly sweet and bitter taste was observed instead (Nomura et al. 2008). In a recent study, Shin et al. (2009) have investigated enzymatic transformation of caffeic acid using aqueous supercritical carbon dioxide under variable pressure at 42°C. Two transglucosylation products were identified by LC/ESI-MS as caffeic acid monoglucoside, with the glucosyl moiety attached to the carboxylic group, and caffeic acid diglucosides (Table IV, Scheme 5). Compared with buffered solution, the use of supercritical carbon dioxide caused a decrease in transfer yield, presumably due to inactivation of sucrose phosphorylase under the high-pressure conditions (Shin et al. 2009).

The Glu^{237}→Gln mutated phosphorylase from *L. mesenteroides* catalyzed glucosyl transfer from Glc1P to acetate and formate at neutral pH (Table IV). Donor substrate hydrolysis occurred at the limit of detection (k_{cat}≈10^{-5} s^{-1}). The wild-type enzyme, by contrast, promoted only the hydrolysis of Glc1P (k_{cat}=2 s^{-1}) but was unable to glucosylate either acetate or formate (Schwarz et al. 2007). Based on Glu^{237}→Gln-catalyzed synthesis of starting material, it was possible for the first time to monitor free acyl group migration in unprotected mono-*O*-acyl D-glucopyranose using one-and two-dimensional *in situ* proton NMR analysis (Brecker et al. 2009).

Production of glucosylglycerol as an industrial fine chemical

Glycosyl glycerols and derivatives thereof are powerful osmolytes (also termed compatible solutes)

Table IV. Glucosylation of carboxylic acceptors using (A) recombinant sucrose phosphorylase from *B. longum*, (B) Glu^{237}→Gln mutated phosphorylase from *L. mesenteroides* and (C) recombinant sucrose phosphorylase from *S. mutans*. Transfer yields were calculated based on the limiting substrate concentration. Structure elucidation of the transglucosylation product was performed by MS and NMR analysis.

	Donor (w/v)	Acceptor (w/v)	Optimized reaction conditions	Transfer yield	Transglucosylation product	Mass of isolated product[a]	Reference
A	Sucrose, 30%	Caffeic acid, 1%	pH 6.8, 42°C, 18 U mL^{-1}	n.d.	Caffeic acid glucoside Caffeic acid diglucosides	n.d.	Shin et al. (2009)
B	Glc1P, 0.3%	Acetate, 1.5% Formate, 1.1%	pH 7.2, 30°C, 9 μM	>80%	1-*O*-Acetyl α-D-glucopyranose[b] 1-*O*-Formyl α-D-glucopyranose[b]	n.d.	Brecker et al. (2009)
C	Sucrose, 30% Sucrose, 40%	Sodium benzoate, 2% Acetic acid, 2.4%	pH 4.6, 40°C, 160 U mL^{-1} pH 3.5, 37°C, 120 U mL^{-1}	70% >80%	1-*O*-Benzoyl α-D-glucopyranose[b] 1-*O*-Acetyl α-D-glucopyranose[b]	0.2 g, 20 mL 0.2 g, 10 mL	Sugimoto et al. (2007) Nomura et al. (2008)

Glc1P, α-D-glucopyranosyl phosphate; n.d., not documented.
[a]Preparative synthesis differed from optimized reaction conditions. [b]Product transformation into 2-*O*-acyl α-D-glucopyranose and 2-*O*-acyl β-D-glucopyranose due to internal acyl group migration and mutarotation.

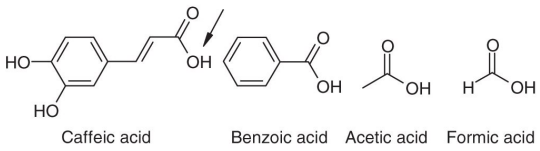

Scheme 5. Structures of glucosyl acceptors having a reactive carboxylic group.

that are produced by various plants, algae and bacteria in adaptation to salt stress and drought (Hincha & Hagemann 2004). 2-*O*-(α-D-Glucopyranosyl)-*sn*-glycerol (GG) is the main compatible solute of cyanobacteria (Fulda et al. 1999). GG has attracted considerable attention for possible use as a moisturizing agent in cosmetics (Thiem et al. 1997) and as a low-calorie sweetener that does not cause tooth decay (Takenaka & Uchiyama 2000). Figure 3 shows a time course of glucosylation of glycerol from sucrose using sucrose phosphorylase from *L. mesenteroides* as the catalyst. Stereochemically pure GG was obtained in high yields of ≥90% donor substrate converted. The biocatalytic process is operated under conditions where the hydrolysis of sucrose is hardly significant. GG is a very poor substrate to be hydrolyzed by sucrose phosphorylase and therefore kinetically stable in the process (Goedl et al. 2008a). The final product concentration is close to 1 M (250 g L^{-1}). The glycerol acceptor is typically used in ≤2.5-fold molar excess over sucrose and is separated (or recycled) at the end of the reaction. GG was obtained in ≥95% purity using chromatography on activated charcoal. The enzyme used in the reaction is recombinantly produced in *Escherichia coli* and can be obtained in useful yield and productivity in

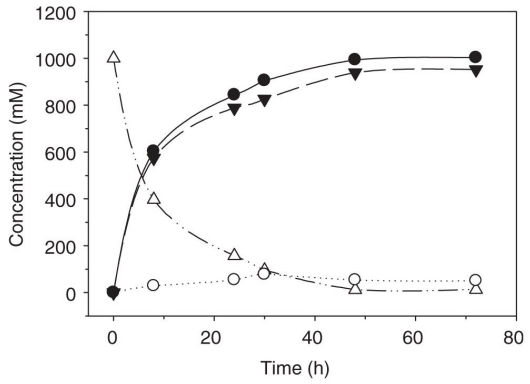

Figure 3. Synthesis of GG using sucrose phosphorylase from *L. mesenteroides*. Reaction conditions: sucrose 1.0 M, glycerol 2.0 M, sucrose phosphorylase 20 U mL^{-1} (crude *E. coli* cell extract containing the recombinant enzyme), at 30°C, in 50 mM MES buffer, pH 7.0. ●, D-Fructose; ○, D-glucose; ▼, GG; Δ, sucrose.

bioreactor culture of the organism (Goedl et al. 2007).

There are several attributes that make the biocatalytic process for GG production outstanding in comparison with relevant transglycosidase-catalyzed conversions reported in the literature (Crout & Vic 1998) (Scheme 6). First of all, using sucrose phosphorylase the competing reaction with water is suppressed kinetically to the extent that hydrolysis of the substrate is prevented completely. Note, however, that a suitable concentration of sucrose (0.3–1.0 M) and glycerol (≥2 M) is needed to achieve this effect. Second, the active site of sucrose phosphorylase provides splendid control over the regioselectivity of glucosyl transfer such that only the desired product is obtained. α-Transglucosidases used for synthesis of GG gave a mixture of glucosyl glycerol regioisomers in which 1-*O*-(α-D-glucopyranosyl)-*rac*-glycerol was the main constituent (Takenaka & Uchiyama 2000; Nakano et al. 2003). Finally, the use of sucrose as a high-energy glucosyl donor, in combination with the substantial kinetic hindrance to the degradation of GG by sucrose phosphorylase, provides a large driving force for an essentially unidirectional reaction, which gives the product in almost quantitative yield. Enzymatic production of GG (Goedl et al. 2008b) was implemented on an industrial scale by the German company bitop AG, and GG was commercialized under the trade name Glycoin. A product termed Glycoin Extremium is available

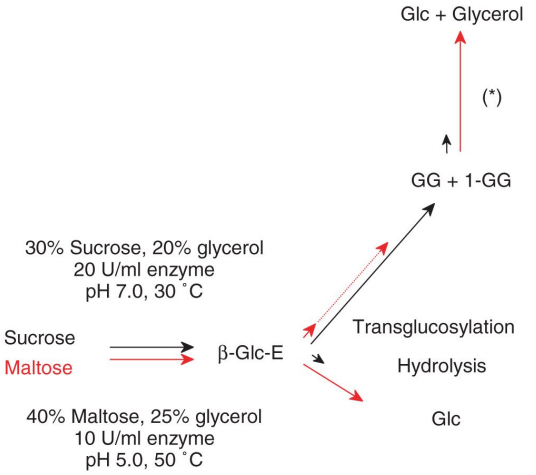

Scheme 6. Comparison of sucrose phosphorylase (black) and α-glucosidase (red) as transglucosylation catalysts for the production of GG. The relative flux through each step of the respective enzymatic reaction was calculated using data from the literature (sucrose phosphorylase: Goedl et al. 2008a; α-glucosidase: Takenaka & Uchiyama 2000) and is indicated by arrow length. Issues related to regioselectivity of glucosyl transfer (dotted lines) and secondary product hydrolysis (*) are indicated. 1-GG, 1-*O*-(α-D-glucopyranosyl)-*rac*-glycerol.

on the market and will be used as an active ingredient for cosmetic formulations (ReedExhibitions 2009).

Conclusions

Sucrose phosphorylase is a well-known enzyme whose splendid features as a glucosylation catalyst may not have been fully appreciated in the past. The enzyme used together with sucrose as the donor substrate provides a highly efficient biocatalytic system for the synthesis of different α-D-glucosides linked to a range of structurally diverse *O*-aglycons. Commercialization of production of GG presents a first case of application of sucrose phosphorylase in industrial fine chemical synthesis.

Acknowledgements

Financial support from the Austrian Science Fund (DK Molecular Enzymology W901-B05 and Project L586-B03) is gratefully acknowledged.

Declaration of interest: The authors report no conflicts of interest. The authors alone are responsible for the content and writing of the paper.

References

Aga H, Yoneyama M, Sakai S, Yamamoto I. 1991. Synthesis of 2-*O*-α-D-glucopyranosyl L-ascorbic acid by cyclodextrin glucanotransferase from *Bacillus stearothermophilus*. Agric Biol Chem 55:1751–1756.

Brecker L, Mahut M, Schwarz A, Nidetzky B. 2009. *In situ* proton NMR study of acetyl and formyl group migration in mono-*O*-acyl D-glucose. Magn Reson Chem 47:328–332.

Cantarel BL, Coutinho PM, Rancurel C, Bernard T, Lombard V, Henrissat B. 2009. The Carbohydrate-Active EnZymes database (CAZy): an expert resource for glycogenomics. Nucleic Acids Res 37:233–238.

Crout DH, Vic G. 1998. Glycosidases and glycosyl transferases in glycoside and oligosaccharide synthesis. Curr Opin Chem Biol 2:98–111.

Doudoroff M. 1943. Studies on the phosphorolysis of sucrose. J Biol Chem 151:351–361.

Doudoroff M, Hassid WZ, Barker HA. 1947. Studies with bacterial sucrose phosphorylase. II. Enzymatic synthesis of a new reducing and of a new non-reducing disaccharide. J Biol Chem 168:733–746.

Empadinhas N, da Costa MS. 2008. To be or not to be a compatible solute: bioversatility of mannosylglycerate and glucosylglycerate. Syst Appl Microbiol 31:159–168.

Fenselau C. 1994. Acyl glucuronides as chemically reactive intermediates. In: Handbook of Experimental Pharmacology. Kauffman FC, editor. Berlin: Springer-Verlag. pp 367–389.

Ferretti JJ, Huang TT, Russell RRB. 1988. Sequence analysis of the glucosyltransferase A gene (*gtfA*) from *Streptococcus mutans* Ingbritt. Infect Immun 56:1585–1588.

Fulda S, Huckauf J, Schoor A, Hagemann M. 1999. Analysis of stress responses in the cyanobacterial strains *Synechococcus* sp. PCC 7942, *Synechocystis* sp. PCC 6803, and *Synechococcus* sp. PCC 7418. Osmolyte accumulation and stress protein synthesis. J Plant Physiol 154:240–249.

Gibson GR, Roberfroid MB. 1995. Dietary modulation of the human colonic microbiota: introducing the concept of prebiotics. J Nutr 125:1401–1412.

Goedl C, Nidetzky B. 2009. Sucrose phosphorylase harbouring a redesigned, glycosyltransferase-like active site exhibits retaining glucosyl transfer in the absence of a covalent intermediate. ChemBioChem 21:2333–2337.

Goedl C, Schwarz A, Minani A, Nidetzky B. 2007. Recombinant sucrose phosphorylase from *Leuconostoc mesenteroides*: characterization, kinetic studies of transglucosylation, and application of immobilised enzyme for production of α-D-glucose 1-phosphate. J Biotechnol 129:77–86.

Goedl C, Sawangwan T, Mueller M, Schwarz A, Nidetzky B. 2008a. A high-yielding biocatalytic process for the production of 2-*O*-(a-D-glucopyranosyl)-*sn*-glycerol, a natural osmolyte and useful moisturizing ingredient. Angew Chem Int Ed 47:10086–10089.

Goedl C, Sawangwan T, Nidetzky B, Mueller M. 2008b. Preparation of 2-*O*-glyceryl-α-D-glucopyranoside from a glucosyl donor and a glucosyl acceptor. PCT International Application WO 2008034158: 25 [assignee, Graz University of Technology].

Hassid WZ, Doudoroff M, Barker HA, Dore WH. 1945. Isolation and structure of an enzymatically synthesized crystalline disaccharide, D-glucosido-L-sorboside. J Am Chem Soc 67:1394–1397.

Hassid WZ, Doudoroff M, Barker HA, Dore WH. 1946. Isolation and structure of an enzymatically synthesized crystalline disaccharide, D-glucosido-D-ketoxyloside. J Am Chem Soc 68:1465–1467.

Hassid WZ, Doudoroff M, Potter AL, Barker HA. 1948. The structure of an enzymatically synthesized reducing disaccharide D-glucosido-L-arabinose. J Am Chem Soc 70:306–310.

Havukkala I. 1991. Trends in xylitology. Trends Glycosci Glycotechnol 3:372–374.

Hincha DK, Hagemann M. 2004. Stabilization of model membranes during drying by compatible solutes involved in the stress tolerance of plants and microorganisms. Biochem J 383:277–283.

Janecek S, Svensson B, Henrissat B. 1997. Domain evolution in the α-amylase family. J Mol Evol 45:322–331.

Kagan BO, Lyatker SN, Tsvasman EM. 1942. Phosphorolysis of sucrose by the cultures of *Leuconoctoc mesenteroides*. Biokhimiya 7:93–108.

Kawasaki H, Narutoshi N, Masaaki O, Kuniko A, Takuo S. 1996. Screening for bacteria producing sucrose phosphorylase and characterization of the enzymes. Biosci Biotechnol Biochem 60:319–321.

Kim SJ, Won YH. 1998. The effect of glycolic acid on cultured human skin fibroplasts: cell proliferation effect and increased collagen synthesis. J Dermatol 25:85–89.

Kitao S, Sekine H. 1992. Transglucosylation catalyzed by sucrose phosphorylase from *Leuconostoc mesenteroides* and production of glucosyl-xylitol. Biosci Biotechnol Biochem 56:2011–2014.

Kitao S, Sekine H. 1994a. α-D-Glucosyl transfer to phenolic compounds by sucrose phosphorylase from *Leuconostoc mesenteroides* and production of α-arbutin. Biosci Biotechnol Biochem 58:38–42.

Kitao S, Sekine H. 1994b. Syntheses of two kojic acid glucosides with sucrose phosphorylase from *Leuconostoc mesenteroides*. Biosci Biotechnol Biochem 58:419–420.

Kitao S, Ariga T, Matsudo T, Sekine H. 1993. The syntheses of catechin-glucosides by transglycosylation with *Leuconostoc mesenteroides* sucrose phosphorylase. Biosci Biotechnol Biochem 57:2010–2015.

Kitao S, Yoshida S, Horiuchi S, Sekine H, Kusakabe I. 1994. Formation of kojibiose and nigerose by sucrose phosphorylase. Biosci Biotechnol Biochem 58:790–791.

Kitao S, Matsudo T, Saitoh M, Horiuchi T, Sekine H. 1995. Enzymatic synthesis of two stable (–)-epigallocatechin gallate-glucosides

by sucrose phosphorylase. Biosci Biotechnol Biochem 59:2167–2169.

Kitao S, Matsudo T, Sasaki T, Koga T, Kawamura M. 2000. Enzymatic synthesis of stable, odorless, and powdered furanone glucosides by sucrose phosphorylase. Biosci Biotechnol Biochem 64:134–141.

Koga T, Nakamura K, Shirokane Y, Mizusawa K, Kitao S, Kikuchi M. 1991. Purification and some properties of sucrose phosphorylase from *Leuconostoc mesenteroides*. Agric Biol Chem 55:1805–1810.

Koga T, Moro K, Matsudo T. 1998. Antioxidative behaviour of 4-hydroxy-2,5-dimethyl-3(2*H*)-furanone and 4-hydroxy-2(or 5)-ethyl-5(or 2)-methyl 3(2*H*)-furanone against lipid peroxidations. J Agric Food Chem 46:946–951.

Kwon T, Kim CT, Lee JH. 2007. Transglucosylation of ascorbic acid to ascorbic acid 2-glucoside by a recombinant sucrose phosphorylase from *Bifidobacterium longum*. Biotechnol Lett 29:611–615.

Lairson LL, Withers SG. 2004. Mechanistic analogies amongst carbohydrate modifying enzymes. Chem Commun 20:2243–2248.

Lee JH, Yoon SH, Nam SH, Moon YH, Moon YY, Kim D. 2006. Molecular cloning of a gene encoding sucrose phosphorylase from *Leuconostoc mesenteroides* B-1149 and the expression in *Escherichia coli*. Enzyme Microb Technol 39:612–620.

Lee JH, Moon YH, Kim N, Kim YM, Kang HK, Jung JY, Abada E, Kang SS, Kim D. 2008. Cloning and expression of the sucrose phosphorylase gene from *Leuconostoc mesenteroides* in *Escherichia coli*. Biotechnol Lett 30:749–754.

Mieyal JJ, Abeles RH. 1972. Disaccharides phosphorylases. In: The Enzymes. Boyer PD, editor. 3rd Ed. New York: Academic Press. pp. 515–532.

Mirza O, Skov LK, Sprogoe D, van den Broek LA, Beldman G, Kastrup JS, Gajhede M. 2006. Structural rearrangements of sucrose phosphorylase from *Bifidobacterium adolescentis* during sucrose conversion. J Biol Chem 281:35576–35584.

Mueller M, Nidetzky B. 2007. The role of Asp-295 in the catalytic mechanism of *Leuconostoc mesenteroides* sucrose phosphorylase probed with site-directed mutagenesis. FEBS Lett 581:1403–1408.

Muto N, Suga S, Fujii K, Goto K, Yamamoto I. 1990. Formation of a stable ascorbic acid 2-glucoside by specific transglucosylation with rice seed α-glucosidase. Agric Biol Chem 54:1697–1703.

Nakano H, Kiso T, Okamoto K, Tomita T, Manan MB, Kitahata S. 2003. Synthesis of glycosyl glycerol by cyclodextrin glucanotransferases. J Biosci Bioeng 95:583–588.

Nomura K, Sugimoto K, Nishiura H, Ohdan K, Nishimura T, Hayashi H, Kuriki T. 2008. Glucosylation of acetic acid by sucrose phosphorylase. Biosci Biotechnol Biochem 72:82–87.

Palleroni NJ, Doudoroff M. 1956. Preparation and properties of D-rhamnulose (6-deoxy-D-fructose) and glucosyl rhamnuloside. J Biol Chem 219:957–962.

JanDekkerInternational. 2009. The spirit of youth. In: Official Show Preview of the In-Cosmetics. Munich, 21–23 April: p. 34.

Robeson JP, Barletta RG, Curtiss 3rd R. 1983. Expression of a *Streptococcus mutans* glucosyltransferase gene in *Escherichia coli*. J Bacteriol 153:211–221.

Russell RRB, Mukasa H, Shimamura A, Ferretti JJ. 1988. *Streptococcus mutans gtfA* gene specifies sucrose phosphorylase. Infect Immun 56:2763–2765.

Sawangwan T, Goedl C, Nidetzky B. 2010. Glucosylglycerol and glucosylglycerate as enzyme stabilizers. Biotechnol J 5:in press.

Sawangwan T, Goedl C, Nidetzky B. 2009. Single-step enzymatic synthesis of (*R*)-2-*O*-α-D-glucopyranosyl glycerate, a compatible solute from micro-organisms that functions as a protein stabiliser. Org Biomol Chem 7:4267–4270.

This paper was first published as an Early Online Article on 10 December 2009.

Scheppach W, Bartram P, Richter A, Richter F, Liepold H, Dusel G, Hofstetter G, Ruthlein J, Kasper H. 1992. Effect of short-chain fatty acids on the human mucosa *in vitro*. JPEN J Parenter Enter Nutr 16:43–48.

Schwarz A, Nidetzky B. 2006. Asp-196→Ala mutant of *Leuconostoc mesenteroides* sucrose phosphorylase exhibits altered stereochemical course and kinetic mechanism of glucosyl transfer to and from phosphate. FEBS Lett 580:3905–3910.

Schwarz A, Brecker L, Nidetzky B. 2007. Acid–base catalysis in *Leuconostoc mesenteroides* sucrose phosphorylase probed by site-directed mutagenesis and detailed kinetic comparison of wild-type and Glu237→Gln mutant enzymes. Biochem J 403:441–449.

Shin MH, Cheong NY, Lee JH, Kim KH. 2009. Transglucosylation of caffeic acid by a recombinant sucrose phosphorylase in aqueous buffer and aqueous-supercritical CO_2 media. Food Chem 115:1028–1033.

Silverstein R, Voet J, Reed D, Abeles RH. 1967. Purification and mechanism of action of sucrose phosphorylase. J Biol Chem 242:1338–1346.

Sprogoe D, van den Broek LA, Mirza O, Kastrup JS, Voragen AG, Gajhede M, Skov LK. 2004. Crystal structure of sucrose phosphorylase from *Bifidobacterium adolescentis*. Biochemistry 43: 1156–1162.

Stam MR, Danchin EG, Rancurel C, Coutinho PM, Henrissat B. 2006. Dividing the large glycoside hydrolase family 13 into subfamilies: towards improved functional annotations of α-amylase-related proteins. Protein Eng Des Sel 19:555–562.

Sugimoto K, Nomura K, Nishiura H, Ohdan K, Nishimura T, Hayashi H, Kuriki T. 2007. Novel transglucosylating reaction of sucrose phosphorylase to carboxylic compounds such as benzoic acid. J Biosci Bioeng 104:22–29.

Takenaka F, Uchiyama H. 2000. Synthesis of α-D-glucosylglycerol by α-glucosidase and some of its characteristics. Biosci Biotechnol Biochem 64:1821–1826.

Thiem J, Scheel O, Schneider G. 1997. Cosmetic preparations with an effective amount of glycosylglycerides as skin moisturizers. European Patent Application EP 770378: 16 [assignee, Beiersdorf AG].

Tsai LB, Gong GS, Tsao GT. 1980. Sucrose phosphorylase from Clostridium pasteurianum. In: Abstracts of the Annual Meeting of the American Society of Microbiology; Miami Beach, 11–16 May: p. 146.

van den Broek LA, van Boxtel EL, Kievit RP, Verhoef R, Beldman G, Voragen AG. 2004. Physico-chemical and transglucosylation properties of recombinant sucrose phosphorylase from *Bifidobacterium adolescentis* DSM20083. Appl Microbiol Biotechnol 65:219–227.

Vandamme EJ, van Loo J, Machtelinckx L, de Laporte A. 1987. Microbial sucrose phosphorylase: fermentation process properties, and biotechnical applications. In: Advances in Applied Microbiology. Laskin AI, editor. Vol. 32. New York: Academic Press. pp. 163–201.

Voet JG, Abeles RH. 1970. Mechanism of action of sucrose phosphorylase. Isolation and properties of a β-linked covalent glucose-enzyme complex. J Biol Chem 245:1020–1031.

Weimberg R, Doudoroff M. 1954. Studies with three bacterial sucrose phosphorylases. J Bacteriol 68:381–388.

Yoon SH, Robyt JF. 2003. Study of the inhibition of four α-amylase by acarbose and its 4^{IV}-α-maltohexaosyl and 4^{IV}-α-maltododecaosyl analogues. Carbohydr Res 338: 1969–1980.

Zhihua L, Hong C, Jing H. 2009. Antiviral therapy of chronic hepatitis B with nucleotide analogs. Anti Infect Agents Med Chem 8:102–113.

3 Regioselective *O*-glucosylation by sucrose phosphorylase: a promising route for functional diversification of a range of 1,2-propanediols.

Christiane Luley-Goedl[a], Thornthan Sawangwan[a], Lothar Brecker[b], Patricia Wildberger[a] and Bernd Nidetzky[a,*]

[a] Institute of Biotechnology and Biochemical Engineering, Graz University of Technology Petersgasse 12/1, A-8010 Graz, Austria, Phone: +43 316 873 8400, Fax: +43 316 873 8434, e-mail: bernd.nidetzky@tugraz.at

[b] Institute of Organic Chemistry, University of Vienna, Währingerstrasse 38, A-1090 Vienna, Austria

Accepted at Carbohydrate Research.

Graphical abstract

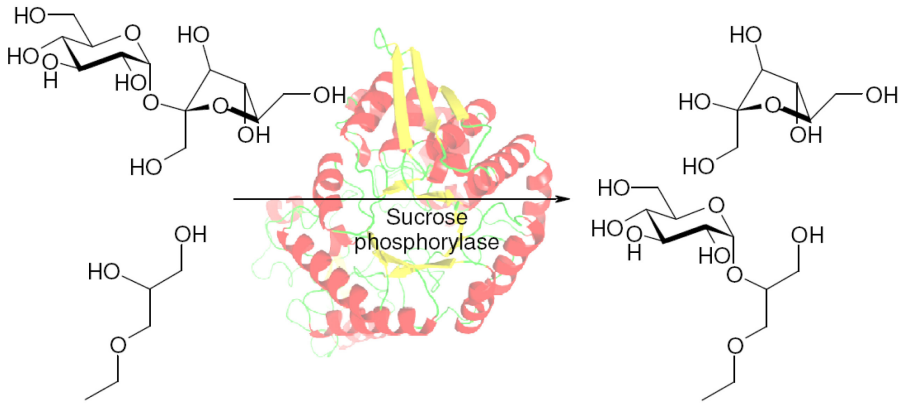

3.1 Abstract

1,2-Propanediol and 3-aryloxy/alkyloxy derivatives thereof are bulk commodities produced directly from glycerol. Glycosylation is a promising route for their functional diversification into useful fine chemicals. Regioselective glucosylation of the secondary hydroxyl in different 1,2-propanediols was achieved by a sucrose phosphorylase-catalyzed transfer reaction where sucrose is the substrate and 2-*O*-α-D-glucopyranosyl products are exclusively obtained. Systematic investigation for optimization of the biocatalytic synthesis included prevention of sucrose hydrolysis, which occurs in the process as a side reaction of the phosphorylase. In addition to "nonproductive" depletion of donor substrate, the hydrolysis also resulted in formation of maltose and kojibiose (up to 45%) due to secondary enzymatic glucosylation of the glucose thus produced. Using 3-ethoxy-1,2-propanediol as acceptor substrate (1.0 M), the desired transfer product was obtained in about 65% yield when employing a moderate (1.5-fold) excess of sucrose donor. Loss of glucosyl substrate to "glucobiose" by-products was minimal ($< 7.5\%$) under these conditions. The reactivity of other acceptors decreased in the order, 3-methoxy-1,2-propanediol > 1,2-propanediol > 3-allyloxy-1,2-propanediol > 3-(*o*-methoxyphenoxy)-1,2-propanediol > 3-*tert*-butoxy-1,2-propanediol. Glucosylated 1,2-propanediols were not detectably hydrolyzed by sucrose phosphorylase so that their synthesis by transglucosylation occurred simply under quasi-equilibrium reaction conditions.

Keywords: Biocatalysis; glycosides; sucrose phosphorylase; glucosylation; 2-*O*-α-D-glucopyranosyl 1,2-propanediol

3.2 Introduction

Due to the large amounts of glycerol accumulating as by-product of bio-diesel production, there is currently high interest in the chemical industries to develop routes for efficient transformation of this "process residue" into useful commodities.[1,2] 1,2-Propanediol and 3-aryloxy/alkyloxy derivatives thereof (Scheme 1A) are bulk products obtained through immediate follow-up chemistry on glycerol.[3] There are diverse technological uses for these compounds, including applications as food additive, as anti-freeze and de-icing agent, and as (chiral) building blocks for fine chemical synthesis.[4,5] Cosmetics is another field where 1,2-propanediols could play a significant role, as moisturizing ingredients for example. However, because 1,2-propanediol causes skin irritation,[6] its application in cosmetic formulations is currently restricted. Glycosylation could be a very useful and general approach with which to enhance the bio-compatibility of the 1,2-propandiols. It could also promote a functional diversification of these compounds such that entirely novel fields of use are opened up. Application as pesticide in weed control is an interesting example. The 1-*O*-α-D-cellobioside of 1,2-propanediol (*rhynchosporoside*) is a host-selective phytotoxin in *Rhynchosporium secalis*, the causal agent of scald disease of barley.[7] A non-natural analogue in which the secondary hydroxyl was glycosylated showed similar plant toxicity as the authentic rhynchosporoside.[8]

Despite its potentially useful effect upon product properties, glycosylation is by no means a routine chemical modification of small molecules.[9] Control of reactivity and selectivity is specially important during glycoside synthesis. Because the strength of biocatalysis lies in coping with exactly these issues of a chemical transformation, enzymes are often the preferred choice of glycosylation catalyst.[10] However, a previously reported galactosylation of 1,2-propanediol catalyzed by β-galactosidase took place with poor regioselectivity and gave only modest yields.[11] Considering the expected value of structurally well defined glycosylated 1,2-propanediols, we therefore examined a transformation catalyzed by sucrose phosphorylase where sucrose is the glucosyl donor substrate and the used 1,2-propanediol is the acceptor. The specificity of enzyme with respect to the 1,2-propanediols in Scheme 1A was unknown.[12] However, two recent papers showing regioselective glucosylation of

glycerol[13] and glycerate[14] by the phosphorylase strongly promoted this investigation. A high-yielding biocatalytic glucosylation of **3** into 3-ethoxy 2-*O*-α-D-glucopyranosyl 1,2-propanediol (**3a**, Scheme 1B) is described. Transformation in a single enzyme-catalyzed step is generally applicable to the compounds in Scheme 1A and proceeds with splendid regioselectivity, irrespective of reactivity differences across the acceptor series used. Detailed analysis of the complex enzymatic reaction, which in addition to desired glucosyl transfer also involves donor substrate hydrolysis and secondary glucosylation of hydrolysis product (glucose), supported design of the overall biocatalytic conversion for optimum product yield (65% based on **3** consumed).

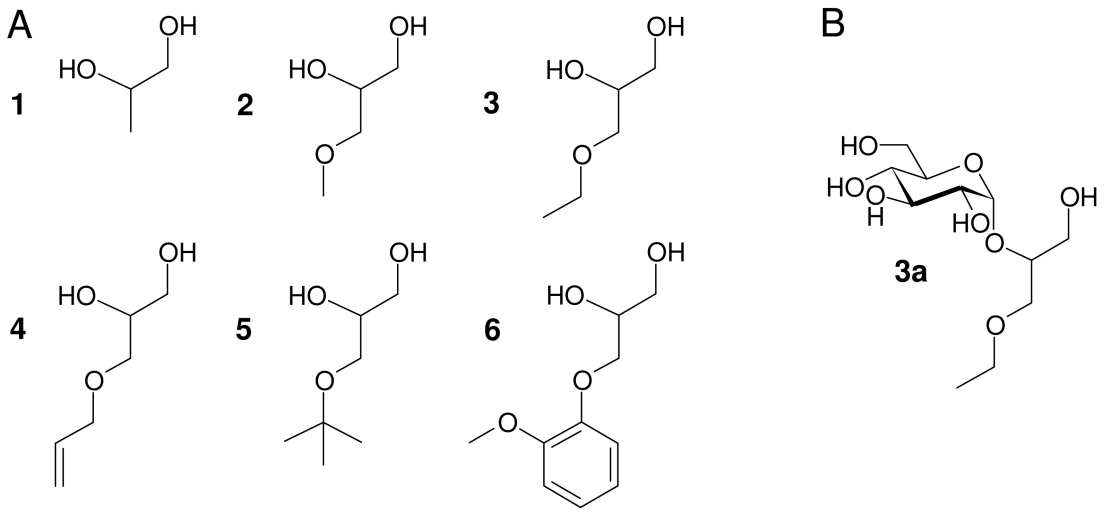

Scheme 1: A) 1,2-Propanediols used in this study. **1**, 1,2-Propanediol; **2**, 3-methoxy-1,2-propanediol; **3**, 3-ethoxy-1,2-propanediol; **4**, 3-allyloxy-1,2-propanediol; **5**, 3-*tert*-butoxy-1,2-propanediol; **6**, 3-(*o*-methoxyphenoxy)-1,2-propanediol. B) Glucosylated product structure of the most efficient acceptor **3**. **3a**, 3-Ethoxy-2-*O*-(α-D-glucopyranosyl)-propanediol.

3.3 Results and discussion

The natural reaction catalyzed by sucrose phosphorylase is the reversible transformation of sucrose and phosphate into α-D-glucose 1-phosphate and D-fructose. In the absence of phosphate, however, alternative glucosyl acceptors can take part in the conversion. Scheme 2 shows the enzymatic reaction resulting in glucosyl transfer from sucrose (donor) to the reactive alcohol group of a suitable acceptor molecule. The absolute stereoselectivity of the enzyme for α-anomeric glucosylation is dictated by the double displacement-like

catalytic mechanism in which a β-configured glucosyl enzyme intermediate has a pivotal role.[15,16] Regioselectivity with respect to different acceptor hydroxyls would seem to reflect requirements of the acceptor binding site of the enzyme. In sucrose phosphorylase, however, the role of the second hydroxyl of the reactive diol moiety in acceptor substrates like fructose,[16] xylitol,[17] glycerol[13] and glycerate[14] appears to be directly auxiliary to catalysis. The crystal structure of an enzyme-sucrose complex of the phosphorylase from *Bifidobacterium adolescentis*[16] supports the idea that the second adjacent hydroxyl facilitates optimum alignment of the catalytic groups of the enzyme relative to the secondary acceptor hydroxyl, which is now the site of the substrate exclusively undergoing reaction.[18] Scheme 2 implies that prevention of donor substrate hydrolysis and thus the accumulation of glucose could represent an important component of reaction optimization (see later). Glucose is a strong inhibitor of sucrose phosphorylase that competes with sucrose for binding to the free enzyme ($K_i \approx 0.5$ mM).[19] Moreover, as described later and shown in literature[20], glucose can also bind where fructose normally binds and serves as alternative glucosyl acceptor substrate (Scheme 2) leading to secondary glucosylation which is a highly undesirable accompaniment.

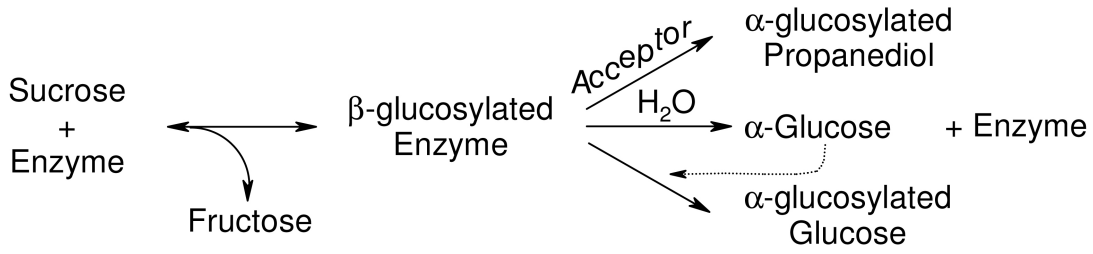

Scheme 2: Mechanism of transglucosylation catalyzed by sucrose phosphorylase, and possible reactions occurring in a biocatalytic conversion of sucrose in the presence of a suitable acceptor. α-D-Glucose is the product of hydrolysis. However α- and β-D-glucose can serve as acceptor in a secondary glucosylation reaction.

3.3.1 Reactivity of different 1,2-propanediols.

Sucrose phosphorylase was incubated for 72 h in the presence of sucrose and either one of the acceptors shown in Scheme 1 (0.3 M each). Analysis of the product mixture by NMR

or HPLC (Table 1) revealed formation of glucosyl transfer product in useful (**2, 3**) to only modest yields (*other acceptors*). However, most (∼90%) of the sucrose initially present had been used up in all reactions at the time of the analysis. The order of acceptor reactivity was **3** > **2** > **1** > **4** > **6** > **5**, indicating that the 3-aryloxy/alkyloxy side chain of 1,2-propanediols was well compatible with acceptor function in the phosphorylase reaction. With each acceptor, glucosyl transfer occurred to the secondary hydroxyl (see Supplementary Information for relevant NMR data), with a possible reaction of the primary hydroxyl being below the detection limit of the analytical method used. The acceptors used in Table 1 were racemic mixtures of *R* and *S* antipodes. Using isolated enantiomers of **1** we found that *R* and *S* forms displayed identical reactivities toward glucosylated sucrose phosphorylase (Table 1). This result is consistent with previous findings showing that the enzyme utilizes *R* and *S*-glycerate as glucosyl acceptors[14] and supports the notion of a highly regioselective transglucosylation catalyzed by sucrose phosphorylase in which, however, enantiomeric discrimination of acceptor alcohols is small. Due to the enzyme's broad acceptor specificity[12] and relatedly to the conformational flexibility of its acceptor binding site[16], evaluation of structural features of the 3-aryloxy/alkyloxy side chain on the enantioselectivity was beyond the scope of this work. Low acceptor enantioselectivity is quite common among transglycosidases.[10c−e,21] It does not, however, compromise the synthetic utility of sucrose phosphorylase in the glucosylation of 1,2-propanediols. As bulk chemicals, the 1,2-propanediols are likely to be available in racemic form, and complete utilization of the acceptor alcohol, that is, reaction of both its *R* and *S* antipodes will be desired. For glucosylation of 1,2-propanediols, therefore, regioselectivity of the biotransformation was the decisive feature.

An unexpected finding of the transglucosylation experiments just described was that glucobioses (maltose, 4-*O*-α-D-glucopyranosyl glucose, kojibiose; 2-*O*-α-D-glucopyranosyl glucose) were formed in large amounts, exceeding in almost all cases the amount of the desired transfer product (Table 1; see Roslund et al.[22] for chemical shift assignment). Production of either maltose or kojibiose had not been observed previously during glucosylation of glycerol[13] and glycerate[14] under otherwise similar reaction conditions. Earlier work of

Kitao et al.[20] had however shown that either "glucobiose" can be formed by a sucrose phosphorylase-catalyzed transglucosylation.

Table 1: Product distribution resulting from conversion of sucrose in the presence of different 1,2-propanediol acceptors. Analytical yields, based on sucrose converted, are given.

Acceptor	2-*O*-α-D-Glucosyl 1,2-propanediol product		Glucobiose product
	NMR [%]	HPLC [%]	NMR [%]
1	6	8, 9.5[a], 7.5[b]	18
2	12	11	17
3	22	26	15
4	5	4	21
5	1	0	22
6	6	n.d.	14

Reaction mixtures (1 mL) were incubated at 30°C and 550 rpm for 72 h using equimolar concentrations of 0.3 M. [a]Product yield obtained in conversion with the pure *R*-enantiomer. [b]Product yield obtained in conversion with the pure *S*-enantiomer. n.d., not determined. The glucobiose product consisted of maltose and kojibiose which were present in approximately equimolar concentrations.

3.3.2 Reaction optimization

Preventing hydrolysis of sucrose and glucosyl transfer to glucose.

Under the standard reaction conditions used for acceptor screening, hydrolysis was a preponderant path of donor substrate conversion (Scheme 2), strongly hampering synthesis. Using **3** as acceptor, about 36% of the sucrose utilized was hydrolyzed by the phosphorylase (Table 2). The concentration of **3a** was just half that of the glucose released. A gradual increase in the initial molar excess of sucrose over the constant acceptor concentration of 0.3 M resulted in substantial (up to 2.6-fold) enhancement of **3a** formation. A product yield of 50% (based on initial acceptor concentration) was obtained. Glucose production also increased as the sucrose level was raised. However, the portion of the converted donor substrate that was lost to hydrolysis decreased markedly in response to an increase in the initial concentration of sucrose. The molar distribution of products (**3a**, glucose) in Table 2 implies that the overall selectivity of the β-glucosyl enzyme intermediate for reaction with **3** as compared to reaction with water was significantly enhanced at high sucrose concentration. It should be noted, therefore, that even at the highest substrate concentra-

tion used (1.5 M), glucosylation of sucrose was not observed! A particular disadvantage of other transglycosylation catalysts described in literature is that substrate competes strongly with external acceptor to become glycosylated in the enzymatic reaction.

Table 2: Product distribution resulting from conversion of sucrose in the presence of **3**. Data are from HPLC analysis and are based on the limiting concentration of donor sucrose or [a]acceptor **3**.

Sucrose	**3**	**3a**		Glucose	
[M]	[M]	[mM]	[%]	[mM]	[%]
0.3		62	21[a]	107	36
0.5		89	30[a]	165	33
0.8	0.3	98	33[a]	204	26
1.0		121	40[a]	225	23
1.5		161	54[a]	207	14
	0.3	72	24	107	36
	0.5	110	37	93	31
	0.8	200	66	70	23
0.3	1.0	219	73	55	18
	1.2	228	76	50	17
	1.5	260	87	37	12

Reactions mixtures (1 mL) were incubated at 30°C and 550 rpm for 24 h.

Table 2 further shows the effect of variation of the concentration of **3** upon production of **3a** under conditions where sucrose was supplied at a constant concentration of 0.3 M. As expected from the proposed kinetic mechanism of the phosphorylase (Scheme 2), hydrolysis of donor substrate was increasingly suppressed as the acceptor concentration was raised. Using 1.5 M of **3**, that is a 5-fold molar excess of acceptor over donor, the yield of **3a** was ∼90% based on the limiting concentration of sucrose. Because the remainder substrate was converted via hydrolysis (Table 2), we can calculate that glucosylated phosphorylase showed a 9-fold preference for reaction with **3** as compared to reaction with water under the conditions used. The yield of **3a** displayed a roughly linear dependence on the acceptor concentration, suggesting that binding of **3** to the β-glucosyl enzyme intermediate was weak and reaction to give **3a** had to occur from a rather unstable encounter complex. By way of comparison, the apparent binding constant (K_M) for fructose is ∼20 mM, indicating that in contrast to **3**, relatively low concentrations of the natural acceptor substrate are sufficient to saturate the glucosylated phosphorylase.

Maximizing the productivity of 3a.

Results in Table 2 indicate that high concentrations of both sucrose and **3** promote formation of **3a**. Figure 1 (panel A) shows results of experiments designed to identify optimum initial concentrations for each substrate, aiming at a maximum final **3a** concentration. Using 1.0 M of **3** and a slight (1.5-fold) molar excess of sucrose, we obtained about 0.65 M of **3a**. The enzymatic reaction was performed at the limit of solubility of substrates so that further increase in either one concentration would have resulted in phase separation. Production of **3a** was lowered in a biphasic system, partly due to instability of sucrose phosphorylase under these conditions (data not shown).

Figure 1 (panel B) depicts a time course of **3a** production applying the optimized substrate concentrations. The different reactions involved in the overall substrate conversion (Scheme 2) took place in the first 44 h of the biocatalytic process. Formation of **3a** continued after this time at a sluggish rate, and the synthesis can be considered to have reached quasi-equilibrium after about 44 h. Sucrose phosphorylase had a half-life of 130 h under the conditions used, indicating that enzyme activity was not a factor limiting production of **3a**. Glucose accumulated quickly to a concentration of ∼130 mM and interestingly, remained then at this level throughout. A steady state between hydrolysis and glucosyl transfer to glucose appears to have been reached. NMR data for a sample taken after 44 h confirmed formation of glucobioses in a concentration of about 90 mM (see Figure 1, panel B). The marked decrease in the **3a** production rate (as well as in the associated substrate consumption rates) already after ∼8 h of reaction may thus have been caused by glucose inhibition. However, considering the attainable product concentrations (0.65 M; 180 g/L), synthesis of **3a** in a single enzyme-catalyzed step seems preparatively highly useful. Prior work has shown clearly the potential for up-scaling of the transglucosylation process to gram scale in the laboratory[13] as well as to industrial manufacturing scale (Glycoin®), and known procedures of downstream processing on activated charcoal[13] should be readily applicable in the isolation of **3a** and related transfer products (Table 1). These aspects of the biotransformation were therefore not further pursued here.

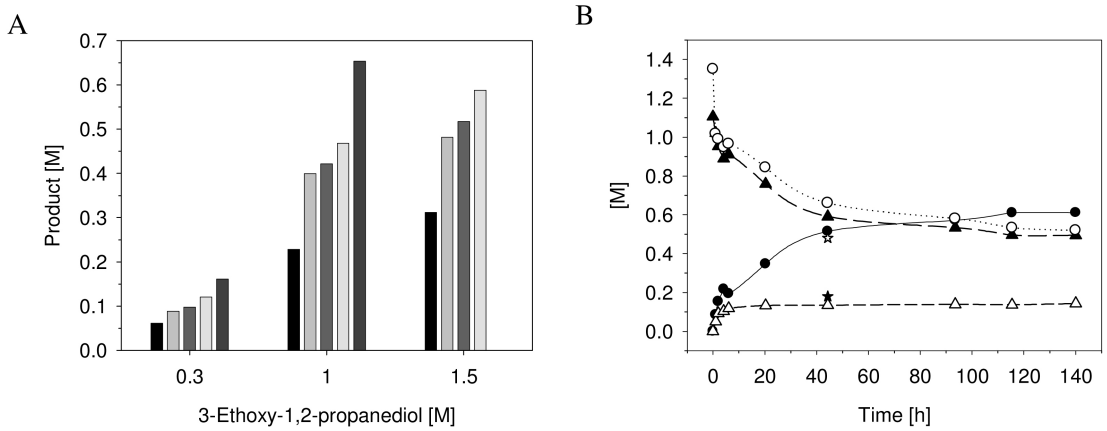

Figure 1: A: Optimization of **3a** production. Coloured bars show the initial sucrose concentration (■ 0.3, ■ 0.5, ■ 0.8, ■ 1.0, ■ 1.5 M). Data are shown for a 72 h-long reaction. B: Time course of **3a** production from 1.5 M of sucrose and 1.0 M of **3**. The symbols show sucrose in a mixture with glucobioses (○), **3** (△), **3a** (●), and glucose (△). The concentrations of sucrose (∗) and glucobioses (⋆), obtained from NMR analysis of a sample taken after 44 h, are indicated separately.

3.3.3 Interpretation of optimization results.

The suggestion from Table 2 that formation of glucose and the consequential formation of maltose and kojibiose was proportionally decreased at high sucrose concentrations was further examined in a "hydrolysis" experiment where 1.5 M of donor substrate were incubated with sucrose phosphorylase in the absence of external acceptor for 24 h. The product distribution of a sample in which 220 mM sucrose had been converted was 20 mM glucobioses (9%) and 180 mM glucose. By way of comparison, the product mixture obtained from an enzymatic conversion of 1.5 M sucrose in the presence of 1.0 M **5** contained 70 mM glucobioses (28%), 100 mM glucose and 10 mM transglucosylation product. The effect of acceptor substrate upon reaction-selectivity of sucrose phosphorylase (hydrolysis as compared to glucosylation) is not accounted for by the kinetic mechanism in Scheme 2. However, crystallographic evidence for sucrose phosphorylase from *B. adolescentis* reveals that the enzyme exploits conformational flexibility of its acceptor binding site in the accommodation of fructose and phosphate[16], two natural, yet structurally completely different glucosyl acceptor substrates of the phosphorylase. The conformation of glucosylated phosphorylase ready to undergo hydrolysis is not known. Notwithstanding, a possible scenario could be that binding of a poor acceptor like **5** favors the "hydrolytic"

protein conformation of the glucosylated phosphorylase and by accumulation of a high amount of glucose within a short time, glucosyl transfer to glucose is promoted as a competitive secondary glucosylation reaction. The main effect of adding 1.0 M glucose to the reaction of sucrose phosphorylase with sucrose (1.5 M) was inhibition of the enzymatic rate. However, formation of glucobioses was also enhanced (3-fold) as compared to the reference reaction lacking glucose.

Formation of 2-*O*- and 4-*O*-glycosidic isomers of α-D-glucopyranosyl glucose suggests that catalytic glucosyl transfer by the phosphorylase involves two different binding modes for the D-glucose acceptor. Based on the crystallographically characterized interactions of the fructosyl moiety at the acceptor site of the enzyme[16] and by also considering structure-activity relationships for different acceptor substrates of the sucrose phosphorylase,[18] we propose recognition of glucose as shown in Scheme 3. From the similar relative content of maltose and kojibiose in the glucobiose mixture produced by the enzyme, we conclude that there is no clear preference for one particular orientation of glucose at the acceptor site of sucrose phosphorylase.

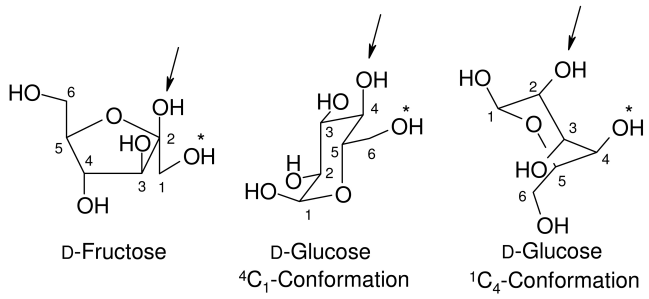

Scheme 3: Proposed modes of productive binding of D-fructose and D-glucose at the glucosyl acceptor site of sucrose phosphorylase. Arrows indicate sites of glucosylation. The hydroxy group marked (*) is important for substrate stabilization in the acceptor binding site.

3.4 Conclusions

This paper reports on efficient regioselective glucosylation of **3** (and related 1,2-propanediols) to yield the corresponding α-D-glucopyranosyl derivatives. Optimization was required to define a useful "operational window" for the biocatalytic transformation whereby suppression of donor substrate hydrolysis and secondary transglucosylation at high substrate

concentrations are main features of the efficient process. It is interesting that side reactions of glucosylated sucrose phosphorylase were of lower relevance during enzymatic glucosylation of glycerol[13] and glycerate[14] as compared to synthesis of **3a**. A notable advantage of sucrose phosphorylase in comparison to the majority of reported transglycosylation catalysts is that the phosphorylase does not glucosylate its substrate sucrose in detectable amounts.[23] Using single-step phosphorylase-catalyzed synthesis, 2-*O*-α-glucosylated 1,2-propanediols might become readily accessible as fine chemicals, thus opening up the possibility for their use in different technological applications and potentially promoting their exploitation as phytotoxin-like active substances to be employed in weed control.[24]

3.5 Experimental

3.5.1 Materials

Sucrose, 1,2-propanediol, 3-methoxy-1,2-propanediol, 3-ethoxy-1,2-propanediol, 3-allyloxy-1,2-propanediol, 3-*tert*-butoxy-1,2-propanediol, 3-(*o*-methoxyphenoxy)-1,2-propanediol - (guaiacol glyceryl ether), and MES buffer (potassium salt) were obtained from Sigma-Aldrich, Vienna, Austria. Sulfuric acid (0.5 M, HPLC grade) was from Carl Roth GmbH & Co, Karlsruhe, Germany. A Cation H Micro-Guard cartridge (30 $\times$ 4.6 mm) and an Aminex HPX-87H column (300 $\times$ 7.8 mm) were from Bio-Rad, Vienna, Austria. All other chemicals used were of highest purity available from Sigma-Aldrich.

3.5.2 Biocatalytic glucosylation

A cell-free extract of recombinant sucrose phosphorylase from *Leuconostoc mesenteroides* was produced in *E. coli* DH10B using reported methods.[25] The enzyme preparation had a specific activity of 40 Units/mg protein, measuring at 30°C the conversion of sucrose and phosphate into α-D-glucose 1-phosphate and fructose, as described elsewhere.[25] Enzyme-catalyzed transformation used a constant phosphorylase activity of 20 Units/mL dissolved in 50 mM MES buffer, pH 7.0. Sucrose and one of the different 1,2-propanediol acceptors were present in the concentrations indicated. The used range of acceptor concentrations was usually limited by solubility. Unless otherwise mentioned, the total volume of the

reaction was 1.0 mL. Incubations were performed, typically for 72 h, in Eppendorf (Vienna, Austria) tubes (1.5 mL) at 30°C using an agitation rate of 550 rpm (Eppendorf Thermomixer comfort). Samples (∼0.1 mL for HPLC; up to ∼1 mL for NMR) were taken at suitable times, heat-treated (99°C; 5 min) to inactivate the enzyme, and centrifuged at 9,520 g to remove precipitated protein prior to further analysis.

3.5.3 Analytics

Measurement of protein concentration and determination of enzyme activity were described elsewhere.[25] HPLC analysis was performed on a LaChrom HPLC system (Merck-Hitachi) equipped with a Cation H Micro-Guard cartridge followed by an Aminex HPX-87H column (300 × 7.8 mm, hydrogen form, Bio-Rad) and a L-7490 RI-detector. Baseline separation was obtained when using 0.005 M sulfuric acid as eluent at a flow rate of 0.6 mL/min and a temperature of 30°C. Authentic (relevant) standards were used for peak identification, and quantification was based on peak area that was suitably calibrated with standards of known concentration dissolved in 50 mM MES buffer pH 7.0. Retention times [min]: sucrose (7.72), glucose (9.14), fructose (10.17), **1** (16.84), **2** (15.30), **3** (16.77), **4** (18.89) and **5** (19.39). Samples for NMR analysis were freeze-dried and dissolved in D_2O. All spectra were recorded on a Bruker DRX-400 AVANCE spectrometer (Bruker, Rheinstetten, Germany) at 300 K and 400 MHz (^{1}H) or 100 MHz (^{13}C) using the Bruker Topspin 2.1 software. Acetone was used as external standard for ^{1}H (δ_H 2.225) and ^{13}C (δ_C 30.89) measurements. For further experimental details see Supplementary Methods.

3.5.4 Calculations

The mass balance for the enzymatic conversion was usually based on measurements of decrease in concentration of free acceptor substrate. Unless mentioned, product yield was calculated based on the initial concentration of the limiting substrate (donor or acceptor). In certain cases, yield was based on the concentration of substrate converted.

Acknowledgements

Financial support from the Austrian Science Fund (Project L586-B03) is gratefully acknowledged. We thank Anne Grady (visiting student from South Dakota) for her experimental contribution.

3.6 References

1. Pagliaro, M.; Ciriminna, R.; Kimura, H.; Rossi, M.; Della Pina, C. *Angew. Chem. Int. Ed. Engl.*, **2007**, 46, 4434-4440.
2. Kenar, J. A. *Lipid Technol.*, **2007**, 19, 249-253.
3. Behr, A.; Eilting, J.; Irawadi, K.; Leschinski, J.; Lindner, *F. Green Chem.*, **2008**, 10, 13-30.
4. Fan, X.; Burton, R. *Open Fuels Energy Sci. J.*, **2009**, 2, 100-109.
5. Bennett, G. N.; San, K. Y. *Appl. Microbiol. Biotechnol.*, **2001**, 55, 1-9.
6. Funk, J. O.; Maibach, H. I. *Contact Dermatitis*, **2006**, 31, 236-241.
7. Auriol, P.; Strobel, G.; Beltran, J. P.; Gray, G. *Proc. Natl. Acad. Sci. USA*, **1978**, 75, 4339-4343.
8. Beltran, J. P.; Strobel, G.; Beier, R.; Bradford, P. M. *Plant Physiol.*, **1980**, 65, 554-556
9. Zhu, X.; Schmidt, R. R. *Angew. Chem. Int. Ed. Engl.*, **2009**, 48, 1900-1934.
10. a) Shaikh, F. A.; Withers, S. G. *Biochem. Cell Biol.*, **2008**, 86, 169-177; b) Bojarova, P.; Kren, V. *Trends Biotechnol.*, **2009**, 27, 199-209; c) Trincone, A.; Giordano, A. *Curr. Org. Chem.*, **2006**, 10, 1163-1193; d) Weijers, C. A. G. M.; Franssen, M. C. R.; Visser, G. M. *Biotechnol. Adv.*, **2008**, 26, 436-456; e) van Rantwijk, F.; Woudenberg-van Oosterom, M.; Sheldon, R. A. *J. Mol. Cat. B:Enzymatic*, **1999**, 6, 511-532; f) de Roode, B. M.; Franssen, M. C. R.; van der Padt, A.; Boom, R. M. *Biotechnol. Prog.*, **2003**, 19, 1391-1402; g) Trincone, A. *Recent Pat. Biotechnol.*, **2010**, 4, 30-47.
11. Crout, D. H.; MacManus, D. A. *J. Chem. Soc.*, Perkin Trans. 1, **1990**, 7, 1865-1868.
12. Goedl, C.; Sawangwan, T.; Wildberger, P.; Nidetzky, B. *Biocatal. Biotransform.*, **2009**, 28, 10-21.
13. Goedl, C.; Sawangwan, T.; Mueller, M.; Schwarz, A.; Nidetzky, B. *Angew. Chem. Int. Ed. Engl.*, **2008**, 47, 10086-10089.
14. Sawangwan, T.; Goedl, C.; Nidetzky, B. *Org. Biomol. Chem.*, **2009**, 7, 4267-4270.
15. Davies, G.; Henrissat, B. *Structure*, **1995**, 3, 853-859.
16. Mirza, O.; Skov, L. K.; Sprogoe, D.; van den Broek, L. A.; Beldman, G.; Kastrup, J. S.; Gajhede, M. *J. Biol. Chem.*, **2006**, 281, 35576-35584.
17. Kitao, S.; Sekine, H. *Biosci. Biotechnol. Biochem.*, **1992**, 56, 2011-2014.
18. Luley-Goedl, C.; Nidetzky, B. *Carbohydr. Res.*, **2010**, doi: 10.1016/j.carres.2010.1003-.1035.

19. Mieyal, J. J.; Abeles, R. H. Disaccharides phosphorylases. In *The Enzymes*, 3rd ed; Boyer, P. D., Ed; Academic Press: New York, **1972**; Vol. 7, pp 515-532.

20. Kitao, S.; Yoshida, S.; Horiuchi, S.; Sekine, H.; Kusakabe, I. *Biosci. Biotechnol. Biochem.*, **1994**, 58, 790-791.

21. Xu, Z. J.; Nakajima, M.; Suzuki, Y.; Yamaguchi, I. *Plant Physiol.*, **2002**, 129, 1285-1295.

22. Roslund, M. U.; Tähtinen, P.; Niemitz, M.; Sjöholm, R. *Carbohydr. Res.*, **2008**, 343, 101-112.

23. van den Broek, L. A.; van Boxtel, E. L.; Kievit, R. P.; Verhoef, R.; Beldman, G.; Voragen, A. G. *Appl. Microbiol. Biotechnol.*, **2004**, 65, 219-227.

24. Vurro, M.; Boari, A.; Evidente, A.; Andolfi, A.; Zermane, N. Pest Manag. *Sci.*, **2009**, 65, 566-571.

25. Goedl, C.; Schwarz, A.; Minani, A.; Nidetzky, B. *J. Biotechnol.*, **2007**, 129, 77-86.

3.7 Supplementary Information

Contents:

Supplementary Methods: NMR spectroscopy.

Supplementary Figures: Chemical structures of glucosylated 1,2-propanediol derivates.

Supplementary Results: NMR shift assignment in glucosylated 1,2-propanediol derivates.

3.7.1 Supplementary Methods

NMR spectroscopy.

All NMR shifts have been determined from the crude reaction mixtures without further purification. Freeze-dried samples were dissolved in D_2O (1 ml) and transferred into 5 mm high precision NMR sample tubes (Promochem, Wesel, Germany). Acetone was used as external standard for ^1H (δ_H 2.225) and ^{13}C (δ_C 30.89) measurements. All spectra were recorded on a Bruker DRX-400 AVANCE spectrometer (Bruker, Rheinstetten, Germany) at 300 K $\pm$ 0.1 K at 400.13 MHz (^1H) or 100.61 MHz (^{13}C) using the Bruker Topspin 2.1 software. For 1D-spectra, 32k data points were acquired using a relaxation delay of 1.0 s. After zero filling to 64k data points and Fourier transformation, spectra with a range of 7,200 Hz (^1H) and 20,000 Hz (^{13}C) were obtained. To determine the 2D COSY, TOCSY, NOESY, HMQC, and HMBC spectra, 128 experiments with 1024 data points each were performed. After linear forward prediction to 256 data points in the f_2-dimension and sinusoidal multiplication in both dimensions, the data was Fourier transformed to obtain 2D-spectra with a range of 4,000 Hz (^1H) and 20,000 Hz (^{13}C).

3.7.2 Supplementary Figures

Supplementary Figure 1. Chemical structures of glucosylated 1,2-propanediol derivates.

1a, 2-*O*-(α-D-glucopyranosyl)-propanediol;

2a, 3-methoxy-2-*O*-(α-D-glucopyranosyl)-propanediol;

3a, 3-ethoxy-2-*O*-(α-D-glucopyranosyl)-propanediol;

4a, 3-allyloxy-2-*O*-(α-D-glucopyranosyl)-propanediol;

5a, 3-*tert*-butoxy-2-*O*-(α-D-glucopyranosyl)-propanediol;

6a, 3-*ortho*-methoxyphenoxy-2-*O*-(α-D-glucopyranosyl)-propanediol.

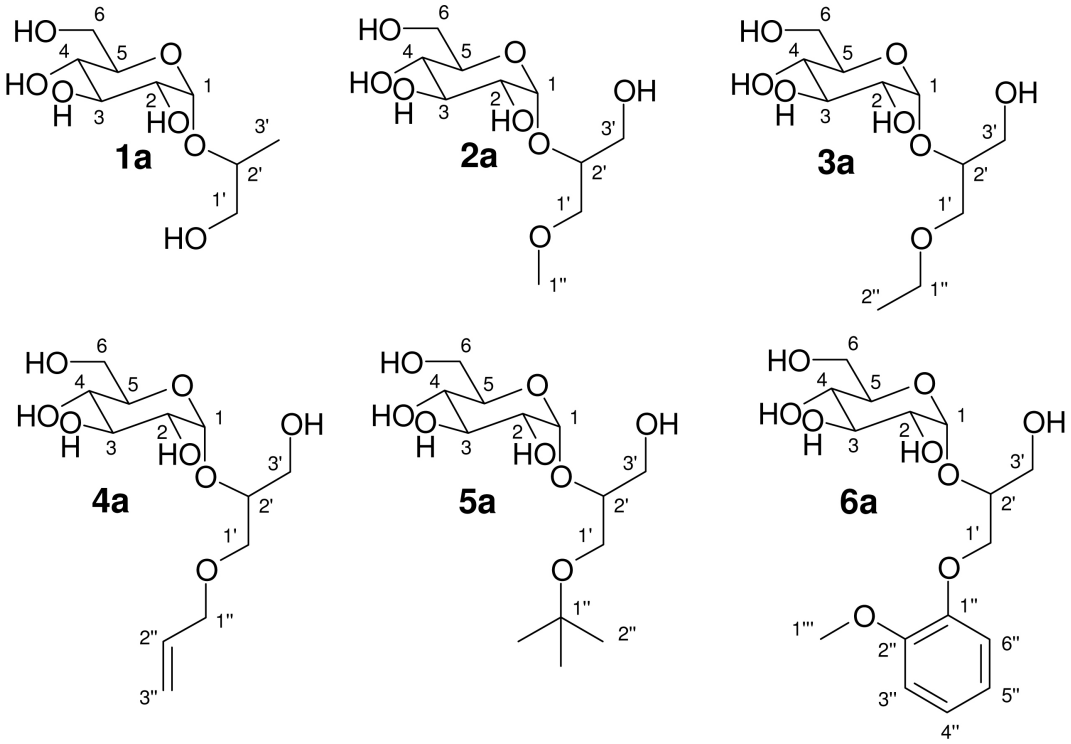

3.7.3 Supplementary Results

Assignment of chemical shifts in 2-*O*-(α-D-glucopyranosyl)-propanediol (1a).
^{1}H NMR (400 MHz, 300 K, D_2O) δ = 5.05 (d, J = 3.8 Hz, 1H, H-1), 3.89 (m, 1H, H-2'), 3.79 (m, 1H, H-6a), 3.78 (m, 1H, H-5), 3.71 (m, 1H, H-3), 3.69 (m, 1H, H-6b), 3.53 (m, 1H, H-1a'), 3.52 (m, 1H, H-2), 3.44 (m, 1H, H-1b'), 3.37 (m, 1H, H-4), 1.15 (d, J = 6.6 Hz, 3H, H-3'); ^{1}3C NMR (100 MHz, 300 K, D_2O) δ = 97.2 (C-1), 74.2 (C-2'), 73.8 (C-3), 72.9 (C-5), 71.2 (C-2), 69.4 (C-4), 67.8 (C-1'), 60.1 (C-6), 19.7 (C-3').

Assignment of chemical shifts in 3-methoxy-2-*O*-(α-D-glucopyranosyl)-propanediol (2a).
^{1}H NMR (400 MHz, 300 K, D_2O) δ = 5.10 (d, J = 3.7 Hz, 1H, H-1), 3.91 (m, 1H, H-2'), 3.81 (m, 1H, H-5), 3.79 (m, 1H, H-6a), 3.74 (m, 1H, H-6b), 3.73 (m, 1H, H-3), 3.70 (m, 1H, H-3a'), 3.62 (m, 1H, H-3b'), 3.53 (m, 1H, H-2), 3.51 (m, 1H, H-1a'), 3.47 (m, 1H, H-1b'), 3.40 (m, 1H, H-4), 3.38 (s, 3H, H-1"); ^{13}C NMR (100 MHz, 300 K, D_2O) δ = 98.3 (C-1), 74.5 (C-2'), 73.8 (C-3), 73.6 (C-1'), 73.5 (C-5), 71.8 (C-2), 69.9 (C-4), 64.3 (C-3'), 60.7 (C-6), 59.0 (C-1").

Assignment of chemical shifts in 3-ethoxy-2-*O*-(α-D-glucopyranosyl)-propanediol (3a).
^{1}H NMR (400 MHz, 300 K, D_2O) δ = 5.13 (d, J = 3.6 Hz, 1H, H-1), 3.88 (m, 1H, H-2'), 3.87 (m, 1H, H-3a'), 3.80 (m, 1H, H-5), 3.78 (m, 1H, H-6a), 3.75 (m, 1H, H-6b), 3.72 (m, 1H, H-3), 3.70 (m, 1H, H-3b'), 3.62 (m, 1H, H-1a'), 3.59 (s, 2H, H-1"), 3.52 (m, 1H, H-2), 3.39 (m, 1H, H-4), 3.45 (m, 1H, H-1b'), 1.17 (s, 3H, H-2"); ^{13}C NMR (100 MHz, 300 K, D_2O) δ = 98.0 (C-1), 74.6 (C-2'), 73.8 (C-1'), 73.6 (C-3), 73.1 (C-5), 71.4 (C-2), 70.0 (C-4), 67.3 (C-1"), 64.3 (C-3'), 60.9 (C-6), 14.6 (C-2").

Assignment of chemical shifts in 3-allyloxy-2-*O*-(α-D-glucopyranosyl)-propanediol (4a).
^{1}H NMR (400 MHz, 300 K, D_2O) δ = 5.96 (ddt, J = 17.3 Hz (d) 11.1 Hz (d), 5.7 (t), 1H,

(H-2"), 5.28 (dm, J = 17.3 Hz, 1H, H-3a"), 5.21 (dm, J = 11.1 Hz, 1H, H-3b"), 5.12 (d, J = 3.7 Hz, 1H, H-1), 4.06 (m, 2H, H-3a"), 3.93 (m, 1H, H-2'), 3.85 (m, 1H, H-3a'), 3.81 (m, 1H, H-5), 3.80 (m, 1H, H-6a), 3.75 (m, 1H, H-6b), 3.73 (m, 1H, H-3), 3.70 (m, 1H, H-3b'), 3.60 (m, 1H, H-1a'), 3.52 (m, 1H, H-2), 3.45 (m, 1H, H-1b'), 3.40 (m, 1H, H-4); ^{13}C NMR (100 MHz, 300 K, D_2O) δ = 133.4 (C-2"), 118.3 (C-3"), 97.9 (C-1), 74.6 (C-2'), 74.0 (C-1'), 73.5 (C-3), 73.2 (C-5), 71.9 (C-1"), 71.5 (C-2), 69.8 (C-4), 64.5 (C-3'), 61.1 (C-6).

Assignment of chemical shifts in 3-*tert*-butoxy-2-*O*-(α-D-glucopyranosyl)-propanediol (5a).

^{1}H NMR (400 MHz, 300 K, D_2O) δ = 5.09 (d, J = 4.0 Hz, 1H, H-1), 3.83 (m, 1H, H-5), 3.80 (m, 1H, H-6a), 3.75 (m, 1H, H-6b), 3.72 (m, 1H, H-3), 3.53 (m, 1H, H-2), 3.39 (m, 1H, H-4), 3.80 (m, 1H, H-3a'), 3.78 (m, 1H, H-2'), 3.70 (m, 1H, H-3b'), 3.60 (m, 1H, H-1a'), 3.45 (m, 1H, H-1b'), 1.22 (s, 9H, H-2"); ^{13}C NMR (100 MHz, 300 K, D_2O) δ = 97.9 (C-1), 74.8 (C-2'), 74.5 (C-1"), 73.7 (C-1'), 73.6 (C-3), 73.4 (C-5), 71.2 (C-2), 69.9 (C-4), 64.4 (C-3'), 60.8 (C-6), 26.9 (C-2").

Assignment of chemical shifts in 3-*o*-methoxyphenoxy-2-*O*-(α-D-glucopyranosyl)-propanediol (6a).

^{1}H NMR (400 MHz, 300 K, D_2O) δ = 6.99 (m, 4H, H-3", H-4", H-5", and H-6"), 5.12 (d, J = 3.6 Hz, 1H, H-1), 4.10 (m, 1H, H-2'), 3.90 (m, 1H, H-3a'), 3.89 (m, 1H, H-5), 3.83 (s, 3H, H-1"'), 3.79 (m, 1H, H-3), 3.75 (m, 1H, H-3b'), 3.72 (m, 1H, H-2), 3.70 (m, 1H, H-6a), 3.60 (m, 1H, H-1a'), 3.52 (m, 1H, H-4), 3.50 (m, 1H, H-1b'), 3.40 (m, 1H, H-6b); ^{13}C NMR (100 MHz, 300 K, D_2O) 149.2 (C-2"), 148.1 (C-1"), 122.4 (C-5"), 122.0 (C-4"), 113.9 (C-6"), 112.8 (C-3"), 98.0 (C-1), 77.4 (C-1'), 74.6 (C-2'), 73.2 (C-3), 73.1 (C-5), 71.7 (C-2), 70.0 (C-4), 60.8 (C-6), 64.5 (C-3'), 56.1 (C-1"').

A Work-flow

A.1 Genetic work

Isolation of pQE30-*Lm*SPase wild-type plasmid from *E. coli* DH 10B

The Wizard Plus SV Miniprep Kit (Promega) was used. The plasmid-DNA from half of an agar plate was eluted in 40 μL of warm water and stored at -20°C.

Agarose gel electrophoresis

Ethidium bromide solution (0.006 μg/mL) was added directly to a 1%-agarose gel. DNA was separated at room temperature and 75 V in 1x TAE-buffer in a BioRad gel system. For quantification and sizing of DNA fragments the Gene Ruler^{TM} DNA Ladder Mix (100-10,000 bp) and the Lambda DNA/HindIII Marker (125-23,130 bp) were used.
After electrophoresis the DNA fragments were detected under UV-light at 312 nm using the BioRad Gel Doc 2000.

Site-directed mutagenesis

The site-directed mutagenesis for introduction of the point mutations Phe52 → Ala (F52A) and Phe52 → Asn (F52N) was performed as described in 1.3.1 using the pQE30-*Lm*SPase wild-type plasmid as template. The amplification product was subjected to parental template digestion by *Dpn*I and transformed into electrocompetent *E. coli* Top10 cells.
The encountered problems during purification of the His-tagged proteins were circumvented by digestion of the *Lm*SPase wild-type and muteins encoding genes from the pQE30 expression vector and ligation into the pASK-IBA7+ expression vector (see Appendix C), which resulted in Strep-tagged wild-type and muteins.
For the introduction of the point mutation Asp82 → Ala (D82A) (see Appendix H), the pASK-IBA7+-*Lm*SPase wild-type plasmid was used as template.

Transformation into electrocompetent *E. coli* Top10 cells

100 μL electrocompetent *E. coli* Top10 cells were mixed with 4 μL of the *Dpn*I restricted

PCR product. Electro-magnetic field was created with the Gene Pulser II (2.5 kV; 5.0 ms). Immediately after electroporation, 900 μL SOC-medium were added and the cells were incubated at 37°C for 1 h and afterwards plated on selective medium.
Single transformants were picked, plated and plasmid-DNA was isolated. Sequencing in both directions was done at the VBC-GENOMICS Bioscience Research GmbH or at LGC Genetics GmbH. Sequence analysis was carried out with Vector NTI.

A.2 Cultivation

Preparation of electrocompetent *E. coli* Top10 cells

Electrocompetent *E. coli* Top10 cells were cultivated in 1 L baffeled shaken flasks at 37°C and 140 rpm using LB-media containing 5 g/L yeast extract, 5 g/L NaCl and 10 g/L peptone until the OD_{600} reached 0.5-0.6. The flasks were put on ice for 20 min and the biomass was transferred into sterile, cooled centrifugation beakers. The cells were harvested by centrifugation at 4°C and 5,000 g for 25 min in a Sorvall RC-5B Refrigerated Superspeed centrifuge. The pellet was resuspended in 60 mL cold, sterile water. For the first washing step, 200 mL cold, sterile water was added to the cells, followed by centrifugation at 4°C and 5,000 g for 25 min. The pellet was resuspended in 10 mL cold, sterile 10% glycerin. For the second washing step, 200 mL cold, sterile 10% glycerin was added to the cells, followed by centrifugation at 4°C and 5,000 g for 25 min. The pellet was resuspended in 30 mL cold, sterile 10% glycerin and the suspension was transferred into a sterile Falcon tube, followed by centrifugation at 4°C and 5000 g for 25 min. Finally, the pellet was resuspened in 4 mL cold, sterile 10% glycerin, aliquoted to 100 μL and frozen with liquid nitrogen.

Heterologous expression of the His-tagged mutants in *E. coli* Top 10

E. coli Top10 cells transformed with the pQE30 expression plasmid were cultivated in 1 L baffeled shaken flasks at 37°C and 110 rpm using LB-medium consisted of 5 g/L yeast extract, 5 g/L sodium chloride, 10 g/L peptone and 115 mg/L ampicillin, until OD_{600} reached 0.5-0.8. The temperature was decreased to 25°C and gene expression was induced

with 0.1 mM isopropyl-ß-D-thio-galactopyranoside (IPTG) for 9 h. The induced cells were harvested by centrifugation at 4°C and 5,000 rpm for 30 min in a Sorvall RC-5B Refrigerated Superspeed centrifuge. The resuspended cells were frozen at -20°C overnight, thawed and the suspension was passed twice through a French pressure cell press (Aminco). Cell debris were removed by centrifugation at 4°C, 14,000 rpm for 45 min. The resulting supernatant was used for further purification of His-tagged *Lm*SPase wild-type and muteins.

Heterologous expression of the Strep-tagged mutants in *E. coli* Top10

The heterologous expression of the Strep-tagged *Lm*SPase wild-type and muteins was performed as described in 1.3.1.

A.3 Purification of *Lm*SPase wild-type and muteins

Purification of the His-tagged muteins did not lead to a pure enzyme preparation (see Appendix I).

Purification of the Strep-tagged wild-type and muteins was performed as described in 1.2.2. The chromatogram of the purification run and the SDS gel are shown in the Supplementary Information.

SDS-PAGE was carried out on a Pharmacia PhastSystem, using pre-cast gradient gels (PhastGel 8-25). The protein bands were visualized by staining with Coomassie Brilliant Blue. The low molecular weight (LMW) standard (GE Healthcare GmbH) consisted of marker proteins with masses of 14.4, 20, 30, 45, 66 and 97 kDa.

A.4 Characterization

All characterization studies were performed with the Strep-tagged *Lm*SPase muteins. The methods of the characterization studies are described in 1.2.3 and 1.2.4. A detailed description of the enzymatic assays is given in Appendix D.

Results of the arsenolysis, hydrolysis and kinetic studies are summarized in 1.4; a detailed description of the results is given in Appendix E (arsenolysis), Appendix G (hydrolysis) and Appendix F (kinetic studies).

B Materials

Pfu DNA Polymerase, Deoxynucleotide Triphosphates (dNTPs), Lambda DNA/*Hind*III marker and *Dpn*I restriction enzyme were obtained from Promega. Restriction endonucleases, T4 DNA ligase and Gene Ruler^{TM} DNA Ladder Mix were purchased from Fermentas. The pASK-IBA7+ vector was obtained from IBA GmbH. The Wizard® Plus SV Minipreps DNA Purification System was obtained from Promega. *E. coli* Top10 cells were used as expression strain for the recombinant pASK-IBA7+ and pQE30 plasmids. Oligonucleotide synthesis was performed at Invitrogen GmbH. DNA sequencing was performed at VBC Biotech Services GmbH and LGC Genomics GmbH. The Strep-Tactin column was purchased from IBA GmbH. The HiPrep 26/10 Desalting column and the Low Molecular Weight Calibration Kit for SDS Electrophoresis were purchased from GE Healthcare GmbH. Phosphoglucomutase from rabbit muscle (PGM), glucose-6-phosphate dehydrogenase from *Leuconostoc mesenteroides* (G6P-DH), hexokinase from *Saccharomyces cerevisiae* (HK) were obatined from Sigma-Aldrich in highest purity available. β-Galactose dehydrogenase S from *E. coli* (Gal-DH) was purchased from Roche Diagnostics GmbH. Galactose-1-phosphate disodium salt was purchased from Carbosynth. All other chemicals were of the highest available purity and were obtained from Sigma-Aldrich.

C Subcloning of *Lm*SPase from pQE30 into pASK-IBA7+

*Lm*SPase wild-type and muteins encoding genes were digested from the pQE30 expression vector (Figure 1) and ligated into the pASK-IBA7+ expression vector (Figure 2). The pASK-IBA7+ vector is equipped with a Strep-Tactin affinity tag, which is fused to the N-terminus of the recombinant protein. This Strep-tag, which is eight amino acids in lenght, binds with high selectivity to Strep-Tactin, an engineered streptavidin. After applying the crude extract on to an Strep-Tactin column and a washing step, elution of the recombinant protein was achieved by addition of desthiobiotin.
For restriction digest Fast Digest *Bam*HI and Fast Digest *Pst*I were used in a 20 μL reaction mix at 37°C for 2 h.

- 2 μL 10x Fast Digest Buffer
- 2 μL pQE30 plasmid DNA (100 ng/μL)
- 1 μL Fast Digest *Bam*HI (10 U/μL)
- 1 μL Fast Digest *Pst*I (10 U/μL)
- 14 μL water

The reaction mix was loaded onto a preparative gel and the corresponding insert (1,600 bp) was excised from the agarose gel. DNA was extracted using the Nucleo Spin Kit from Promega and eluted in 20 μL water at 37°C.
Ligation of the insert into the cut and dephosphorylated pASK-IBA7+ vector was done in a 10 μL reaction mix at 4°C for 16 h.

- 7.5 μL insert (15 ng/μL)
- 0.5 μL vector (90 ng/μL)
- 1 μL 10x ligase buffer
- 1 μL T4-DNA ligase (1-2 U/μL)

The expression plasmid was transformed into *E. coli* Top10 cells and plated on selective LB-Amp-plates. Plasmid-DNA was isolated by MiniPrep (Promega) and a control restriction digest was performed to ensure that the insert and vector were present and had the right size. Finally, the samples were sent for sequencing.

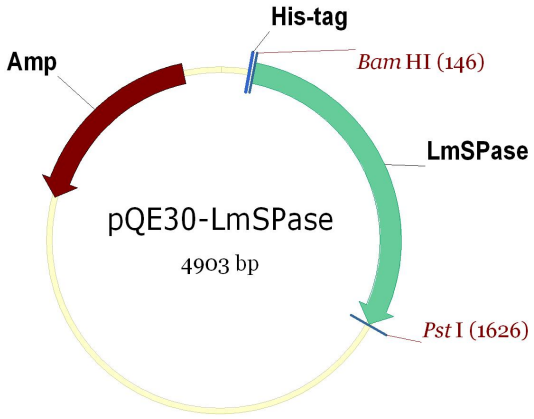

Figure 1: Expression plasmid pQE30-*Lm*SPase. Recombinant *Lm*SPase carries an N-terminal His-tag. The abbreviations indicate His-tag, 6x His-tag coding sequence; *Bam*HI and *Pst*I, restriction sites of the endonucleases; and Amp, β-lactamase coding sequence providing ampicillin resistance.

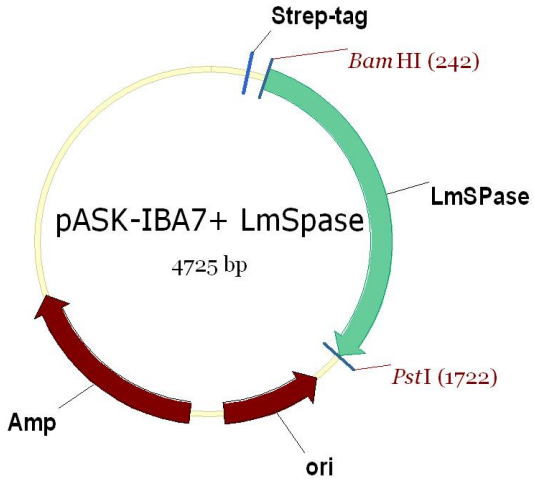

Figure 2: Expression plasmid pASK-IBA7+-*Lm*SPase. Recombinant *Lm*SPase carries an N-terminal Strep-tag. The abbreviations indicate Strep-tag, Strep-Tactin affinity tag; *Bam*HI and *Pst*I, restriction sites of the endonucleases; ori, origin of replication; and Amp, β-lactamase coding sequence providing ampicillin resistance.

D Enzymatic assays

D.1 Activity measurement in phosphorolysis direction

The activity is determined at 30°C using a continuous coupled enzymatic assay, in which production of G1P from sucrose and P_i is coupled to the reduction of NAD^+ in the presence of phosphoglucomutase (PGM) and glucose-6-phosphate dehydrogenase (G6P-DH). One unit of activity (1U) refers to 1 μmol NADH per minute. The standard assay is performed as described elsewhere [1].

$$\begin{aligned}
\text{sucrose} + P_i &\xrightarrow{\text{SPase}} \text{G1P} + \text{D-fructose} \\
\text{G1P} &\xrightarrow{\text{PGM}} \text{G6P} \\
\text{G6P} + NAD^+ &\xrightarrow{\text{G6P-DH}} \text{gluconolacton-6-phosphate} + NADH + H^+ \\
\text{gluconolacton-6-phosphate} &\longrightarrow \text{gluconat-6-phosphate} + H^+
\end{aligned}$$

Test buffer system:

- 50 mM potassium phosphate buffer (pH 7.0)
- 10 mM $MgCl_2$
- 10 mM EDTA
- 5 μM glucose-1,6-biphosphate

Reaction mixture:

- 380 μL test buffer
- 40 μL NAD^+ solution (20 mg/ml)
- 2 μL PGM (850 U/ml in 3 M $(NH_4)_2SO_4$, pH 5.0)
- 2 μL G6P-DH (950 U/ml in 3.2 M $(NH_4)_2SO_4$, 50 mM Tris, 1 mM $MgCl_2$, pH 7.2)
- 10 μL enzyme (optimal 0.5 - 1 U/ml, max. 1.5 U/ml)

The reaction is started by addition of 130 μL sucrose solution (1.1 M in buffer). The formation of NADH with time is measured at 340 nm for 15 min. Calculations are performed

using following equation:

$$c = \frac{\Delta E}{\Delta t} \cdot \frac{V_{total}}{V_{sample} \cdot \epsilon \cdot d} \tag{1}$$

with V_{total}=564 μL; V_{sample}=10 μL; ϵ=6.22 $mM^{-1}cm^{-1}$; and d=1 cm

D.2 Determination of inorganic phosphate concentration

For the activity measurements in synthesis direction, the amount of released phosphate is determined colorimetrically at 850 nm and 30°C [2]. The underlying principle is that phosphate forms a complex with ammonium molybdate in the presence of Zn^{2+} at pH 5, which strongly absorbs ultraviolet light. The phosphomolybdate complex is reduced by ascorbic acid and the chromophore produced shows maximum absorption at 850 nm.

Molybdate reagent:

15 mM ammonium molybdate

100 mM zinc acetate

adjusted to pH 5.0 with concentrated HCl and stored in a polyethylene bottle at room temperature protected from sunlight, otherwise the blank values increase with time.

10% ascorbic acid reagent:

100 g/L sodium ascorbic acid

adjusted to pH 5.0 with 4 M HCl

prepared fresh daily

Test solution:

4/5 of molybdate reagent

1/5 of 10% ascorbic acid reagent

Assay mixture:

30 μL sample or H_2O

470 μL test solution

After 15 min incubation at 25 °C, the absorbance is read at 850 nm against a blank. Calculation of the inorganic phosphate concentration is done using a calibration curve in the range of 0.0 to 1.0 mM phosphate. KH_2PO_4 was used for preparation of standards.

D.3 Glucose measurement

D-glucose is measured using a hexokinase based assay, where D-glucose is converted to G6P by hexokinase (HK) and G6P is subsequently converted to gluconat-6-phosphate by glucose-6-phosphate dehydrogenase (G6P-DH), which is coupled to the reduction of NAD^+ to NADH. The formation of NADH is measured spectrophotometrically at 340 nm and is proportional to the amount of D-glucose.

$$\text{glucose} + \text{ATP} \xrightarrow{\text{HK}} \text{G6P} + \text{ADP}$$

$$\text{G6P} + \text{NAD}^+ \xrightarrow{\text{G6P-DH}} \text{gluconat-6-phosphate} + \text{NADH} + \text{H}^+$$

Solution 1:

70 mM NaH_2PO_4

4 mM $MgSO_4$

1.6 mM ATP

1.6 mM NAD^+

All compounds are dissolved in 40 mL deionized H_2O and adjusted to pH 7.7 with 1 M NaOH and finally made up to 50 mL. Solution 1 is stable for 14 days at 4°C.

Enzyme solution:

HK ($\geq$ 100 U/mL)

G6P-DH ($\geq$ 180 U/mL)

100 mM $MgSO_4$

All compounds are dissolved in 0.6 mL of 50% (w/w) glycerol. The enzyme solution is stable for one month at 4°C.

Assay mixture:

100 μL solution 1

5 μL sample

after mixing, absorbance A_1 is read at 340 nm, 30°C

1 μL enzyme solution is added

after steady-state is reached (5 to 20 min), absorbance A_2 is read

Calculations are performed using following equation:

$$c = \Delta A \cdot \frac{V_{total}}{V_{sample} \cdot \epsilon \cdot d} \tag{2}$$

with $\Delta A = A_2 - A_1$; V_{total}=106 μL; V_{sample}=5 μL; ϵ=6.22 $mM^{-1}cm^{-1}$; and d=1 cm

D.4 Galactose measurement

D-galactose is measured using a galactose dehydrogenase based assay, where galactose is converted to D-galactonate by galactose dehydrogenase (Gal-DH), which is coupled to the reduction of NAD^+ to NADH. The formation of NADH with time is measured spectrophotometrically at 340 nm for 60 min.

$$\text{D-galactose} + NAD^+ \xrightarrow{\text{Gal-DH}} \text{D-galactonate} + NADH$$

Solutions:

100 mM Tris/HCl dissolved in 100 mL deionized H_2O and adjusted to a pH of 8.6 with 1 M HCl

72 mM NAD^+ dissolved in 1 mL deionized H_2O

10 mM galactose dissolved in 2 mL deionized H_2O

0.6 U/mL Gal-DH in 1 M $(NH_4)_2SO_4$

Reaction mixture:

500 μL Tris/HCl, pH 8.6

17 μL NAD^+

17 μL sample

after mixing, absorbance A_1 is read

17 μL Gal-DH

after mxing and incubation for 60 min, absorbance A_2 is read

Calculation of the galactose concentration is done using a calibration curve in the range of 0.5 to 10.0 mM galactose.

D.5 Glucose-1-phosphate measurement

D-glucose-1-phosphate is determined at 30°C using a coupled enzymatic assay, in which production of G1P is coupled to the reduction of NAD^+ in the presence of phosphoglucomutase (PGM) and glucose-6-phosphate dehydrogenase (G6P-DH). One unit of activity (1U) refers to 1 μmol NADH per minute. The standard assay is performed as described elsewhere [1].

$$\begin{aligned} \text{G1P} &\xrightarrow{\text{PGM}} \text{G6P} \\ \text{G6P} + \text{NAD}^+ &\xrightarrow{\text{G6P-DH}} \text{gluconolacton-6-phosphate} + \text{NADH} + \text{H}^+ \\ \text{gluconolacton-6-phosphate} &\longrightarrow \text{gluconat-6-phosphate} + \text{H}^+ \end{aligned}$$

Buffer system:

50 mM Tris/HCl

10 mM $MgCl_2$

10 mM EDTA

5 μM glucose-1,6-biphosphate

dissolved in deionized H_2O and adjusted to a pH of 7.7 with half-concentrated HCl

Reaction mixture:

400 μL buffer system

10 μL NAD^+ solution (20 mg/ml)

2 μL G6P-DH (950 U/ml in 3.2 M $(NH_4)_2SO_4$, 50 mM Tris, 1 mM $MgCl_2$, pH 7.2)

40 μL sample

after mixing and incubation for 5 min, absorbance A_1 is read

2 μL PGM (850 U/ml in 3 M $(NH_4)_2SO_4$, pH 5.0)

after mixing, absorbance A_2 is read, when the reaction has finished

Calculations are performed using following equation:

$$c = \Delta A \cdot \frac{V_{total}}{V_{sample} \cdot \epsilon \cdot d} \tag{3}$$

with $\Delta A = A_2 - A_1$; V_{total}=454 μL; V_{sample}=40 μL; ϵ=6.22 $mM^{-1}cm^{-1}$; and d=1 cm

D.6 Glucose measurement in the presence of fructose

D-glucose in the presence of fructose is determined using a glucose oxidase based assay. According to mutarotation, α-D-glucose is in equilibrium with β-D-glucose which is converted into D-glucono-δ-lactone and hydrogen peroxide by glucose peroxidase (GOD) in the presence of O_2. This conversion is coupled to the oxidation of o-dianisidine by peroxidase (POD). The H_2O_2-dependent formation of coloured product is determined at 405 nm. The standard assay is performed as described elsewhere [3].

$$\alpha\text{-D-glucose} \rightleftharpoons \beta\text{-D-glucose}$$

$$\beta\text{-D-glucose} + H_2O + O_2 \xrightarrow{\text{GOD}} \text{D-glucono-}\delta\text{-lactone} + H_2O_2$$

$$\text{o-dianisidine}_{red} + H_2O_2 \xrightarrow{\text{POD}} \text{o-dianisidine}_{ox} + H_2O$$

Reaction mixture:

50 mM K_2HPO_4

GOD (21 kU/L)

POD (1.5 kU/L)

all compounds are dissolved in 49 mL deionized H_2O

0.79 mM o-dianisidine dihydrochloride is dissolved in 1 mL deionized H_2O and carefully added to the K_2HPO_4 buffer to prevent turbitity

Assay mixture:

100 μL reaction mixture

5 μL sample

the assay mixture is incubated at room temperature for 30 min (protected from light) and absorbance is read at 405 nm.

Calculation of the glucose concentration is done using a calibration curve in the range of 0.5 to 3 mM glucose.

D.7 Measurement of protein concentration

Concentration of the soluble protein is determined using the Bio-Rad Protein Assay. The Bio-Rad Protein Assay is a dye-binding assay in which a differential colour change of a dye occurs in response to various concentrations of protein. The absorbance maximum for an acidic solution of Coomassie® Blue G-250 dye shifts from 465 nm to 595 nm when binding to protein occurs. The Coomassie blue dye binds primarily basic and aromatic amino acid residues, especially arginine.

Protein concentration is determined using the Bio-Rad dye binding assay with BSA as the standard. The sample (20 μL) is mixed with 1000 μL of the 1:5-dilute dye reagent and after 15 min incubation at 25°C the absorbance is measured at 595 nm. Calculation of the concentration is done using the BSA calibration curve in the range of 0.0 to 1.0 mg/mL.

E Arsenolysis

Instead of phosphate, arsenate can be used as alternative glycosyl acceptor substrate. In contrast to the reversible reaction of phosphorolysis, the arsenolysis is irreversible, because the α-glycopyranosyl arsenate (G1As; Gal1As) decomposes hydrolytically, yielding glucose or galactose, arsenate (As_i) and phosphate (P_i), when G1P or Gal1P serve as substrate, respectively.

$$\mathrm{G1P + As_i \xrightarrow{SPase} G1As + P_i}$$

$$\mathrm{G1As + P_i \longrightarrow Glucose + As_i + P_i}$$

$$\mathrm{Gal1P + As_i \xrightarrow{SPase} Gal1As + P_i}$$

$$\mathrm{Gal1As + P_i \longrightarrow Galactose + As_i + P_i}$$

The rate of arsenolysis was determined at 30°C in 50 mM MES buffer, pH 7.0 using discontinuous assays [50 mM arsenate, 50 mM Gal1P or 50 mM G1P, in presence of 0.15 mg/mL enzyme], in which formation of glucose or galactose, was measured (Figure 3; Figure 4). Gal1P and G1P decompose hydrolytically over time, yielding galactose or glucose and phosphate, respectively. Thus, control reactions lacking the enzyme [50 mM arsenate, 50 mM Gal1P or 50 mM G1P] were performed to determine the time-dependent autohydrolysis of the substrate. The reported values, from which the catalytic acitivties were calculated, were corrected for the blank readings.

The released galactose was measured using a galactose dehydrogenase based assay (see Appendix D.4). Calculation of the galactose concentration was done using a calibration curve (Figure 5) in the range of 0.5 to 10 mM galactose. All measurements were performed on the Beckman Coulter DU 800 Spectrophotometer. The released glucose was measured using a hexokinase based assay (see Appendix D.3). Calculation of the glucose concentration was done using a calibration curve (Figure 6) in the range of 0.1 to 10.0 mM glucose. All measurements were performed on the FLUOstar Omega Plate Reader.

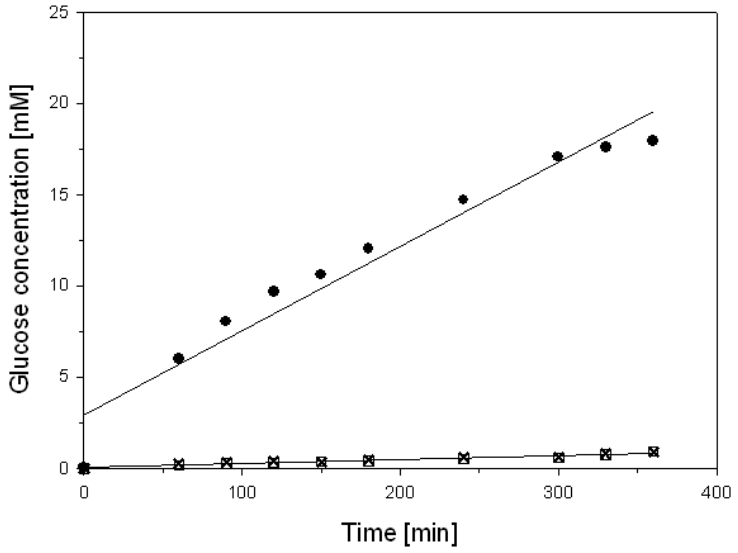

Figure 3: Time-dependent measurements of the G1P arsenolysis catalyzed by *Lm*SPase wild-type (•), F52A (×) and F52N (□). The reported values were corrected for the blank readings.

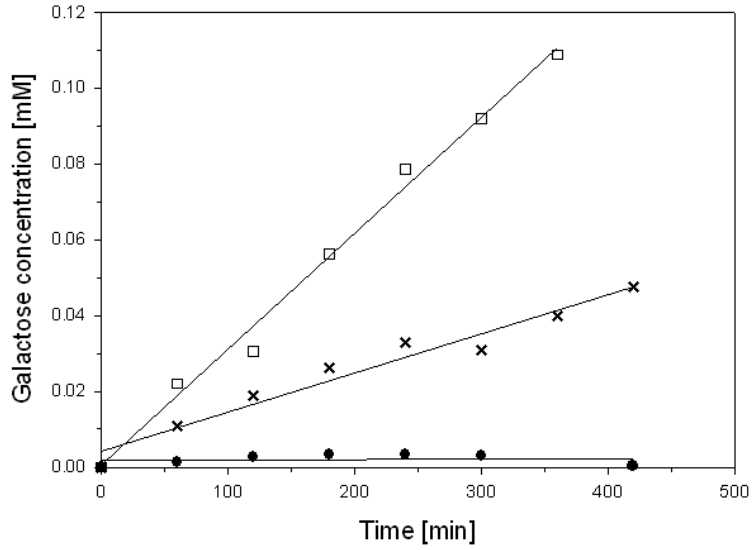

Figure 4: Time-dependent measurements of the Gal1P arsenolysis catalyzed by *Lm*SPase wild-type (•), F52A (×) and F52N (□). The reported values were corrected for the blank readings.

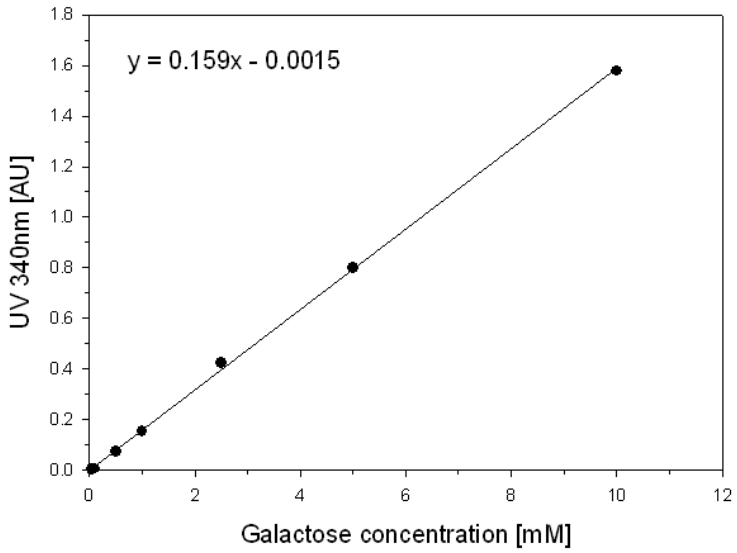

Figure 5: Calibration curve for the galactose dehydrogenase based assay in the range of 0.5 to 10 mM galactose.

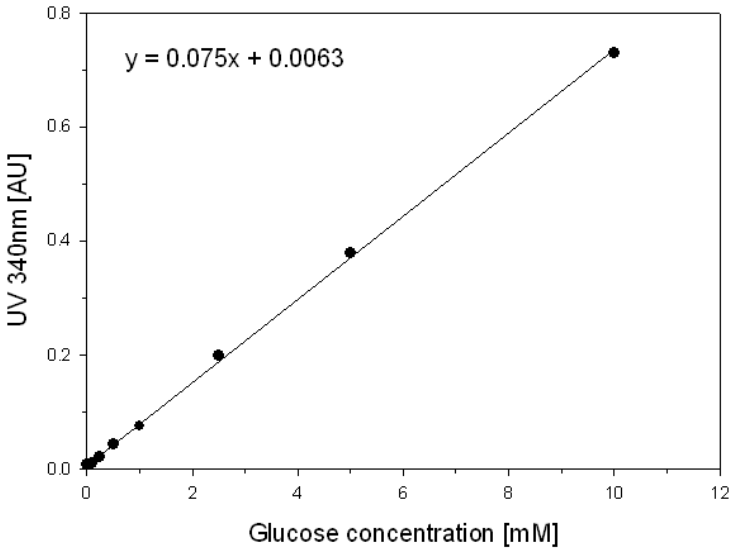

Figure 6: Calibration curve for the glucose hexokinase based assay in the range of 0.1 to 10 mM glucose.

F Kinetic studies

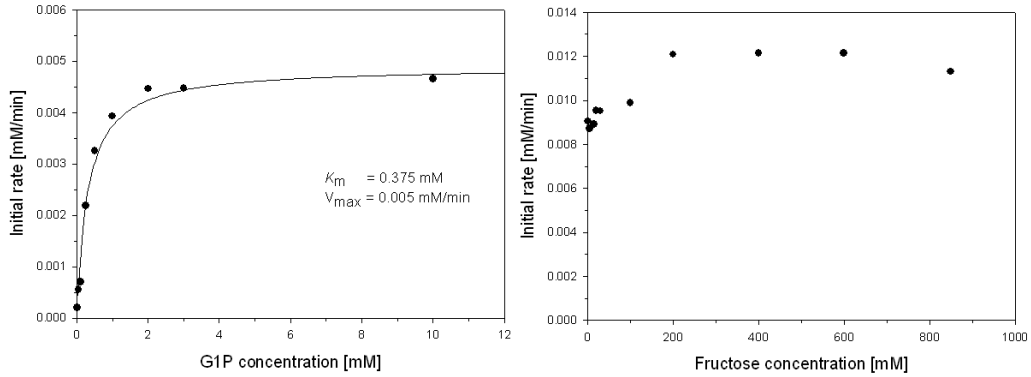

Figure 7: Michaelis-Menten plots for the determination of kinetic parameters in synthesis direction catalyzed by *Lm*SPase-F52A. Initial-rates were determined as function of P_i release using a discontinuous assay. The enzymatic assay was performed in 50 mM MES buffer, pH 7.0 at 30°C and 550 rpm with an enzyme concentration of 0.35 mg/mL at saturating concentrations of 220 mM fructose or 20 mM G1P, respectively.

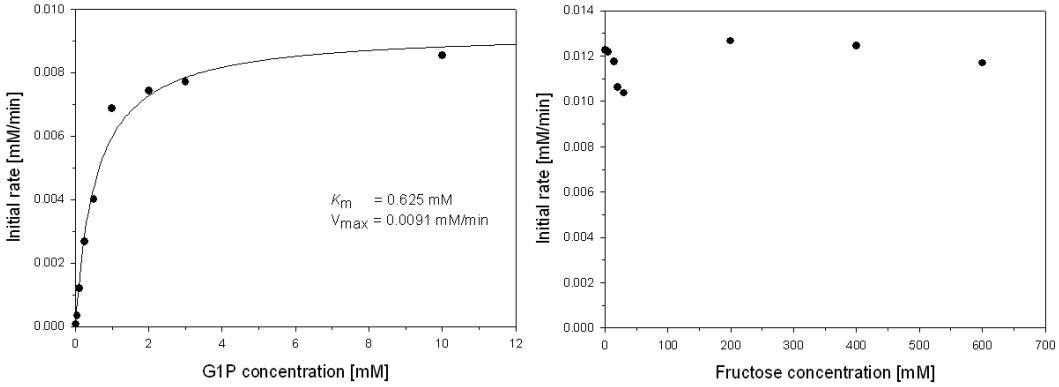

Figure 8: Michaelis-Menten plots for the determination of the kinetic parameters in synthesis direction catalyzed by *Lm*SPase-F52N. Initial-rates were determined as function of P_i release using a discontinuous assay. The enzymatic assay was performed in 50 mM MES buffer, pH 7.0 at 30°C and 550 rpm with an enzyme concentration of 0.35 mg/mL at saturating concentrations of 220 mM fructose or 20 mM G1P, respectively.

The catalytic activity was not altered by varying fructose concentrations, which excludes fructose from taking part in the reaction. The high binding affinity of G1P to the muteins in combination with the non-detectable binding affinity of fructose led to the assumption that the catalytic activity in synthesis direction was completely disrupted and instead of product formation (=sucrose), hydrolysis occured. Thus, the values shown for the G1P

binding affinities are hydrolysis values.

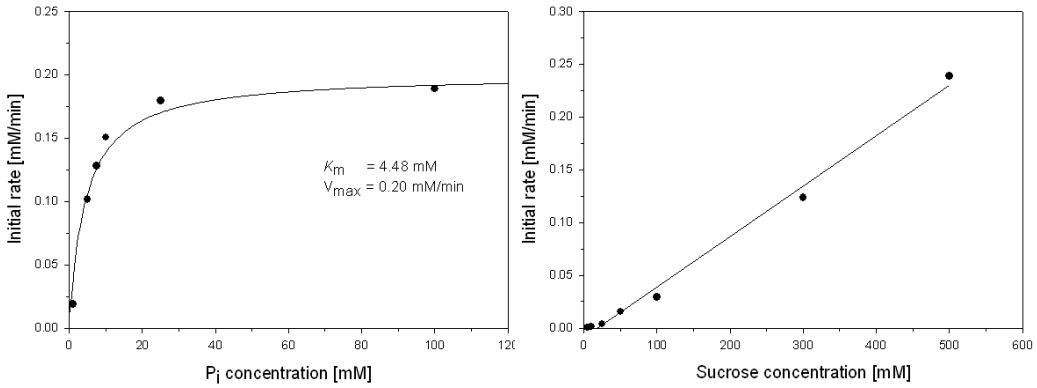

Figure 9: Michaelis-Menten plots for the determination of kinetic parameters in phosphorolysis direction catalyzed by *Lm*SPase-F52A. Initial-rates were determined as function of G1P release using discontinuous assay. The enzymatic assay was performed in 50 mM MES buffer, pH 7.0 at 30°C and 550 rpm with an enzyme concentration of 0.30 mg/mL at saturating concentrations of 500 mM sucrose or 50 mM phosphate, respectively.

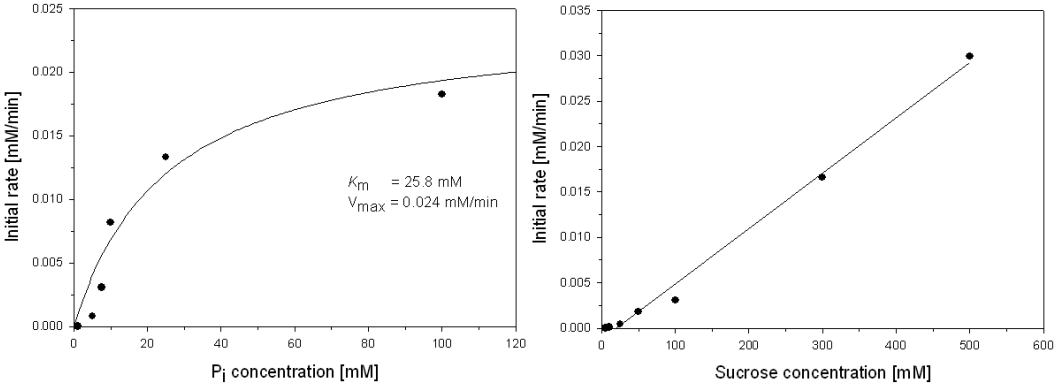

Figure 10: Michaelis-Menten plots for the determination of kinetic parameters in phosphorolysis direction catalyzed by *Lm*SPase-F52N. Initial-rates were determined as function of G1P release using discontinuous assay. The enzymatic assay was performed in 50 mM MES buffer, pH 7.0 at 30°C and 550 rpm with an enzyme concentration of 0.30 mg/mL at saturating concentrations of 500 mM sucrose or 50 mM phosphate, respectively.

G Hydrolysis

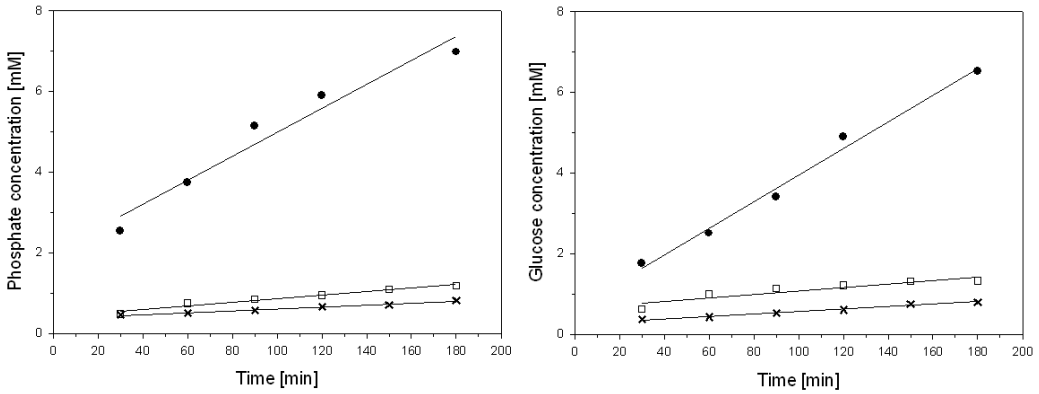

Figure 11: Time-dependent measurements of the G1P hydrolysis catalyzed by *Lm*SPase wild-type (•), F52A (×) and F52N (□). Initial-rates were determined as function of glucose and P_i release using a discontinuous assay. The enzymatic assay was performed in 50 mM MES buffer, pH 7.0 at 30°C and 550 rpm with an enzyme concentration of 0.2 mg/mL for the muteins and 0.02 mg/mL for the wild-type at saturating G1P concentrations of 20 mM.

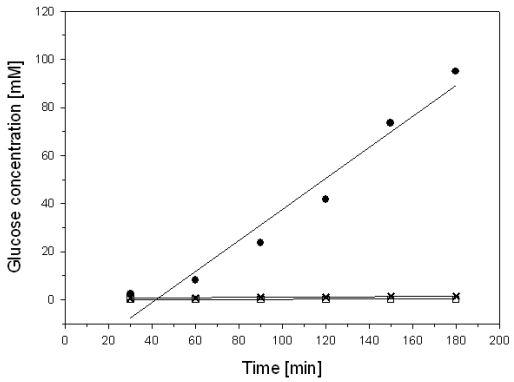

Figure 12: Time-dependent measurements of the sucrose hydrolysis catalyzed by *Lm*SPase wild-type (•), F52A (×) and F52N (□). Initial-rates were determined as function of glucose release using a discontinuous assay. The enzymatic assay was performed in 50 mM MES buffer, pH 7.0 at 30°C and 550 rpm with an enzyme concentration of 0.2 mg/mL at saturating sucrose concentrations of 500 mM.

H *Lm*SPase-D82A

The point mutation D82 → Ala (D82A) was introduced using a two-stage PCR protocol as described in 1.3.1 (reaction cycle: 95°C, 50 s/55°C, 50 s/72°C, 10 min). The used template was the pASK-IBA7+-*Lm*SPase wild-type plasmid (see Appendix C). One complementary pair of oligonucleotide primers was designed to achieve the desired mutation (mismatched bases are underlined):

*Lm*SPase D82A forward: 5'-CTATTTGATGTTTGCTTTCATGATTAACC-3'

*Lm*SPase D82A backward: 5'-GGTTAATCATGAAAGCAAACATCAAATAG-3'

Cultivation and purification of the *Lm*SPase-D82A mutein (Figure 13) was performed as described in 1.3.2. To determine the glucose and galactose transfer activity of the mutant, an arsenolysis study with G1P and Gal1P was performed.

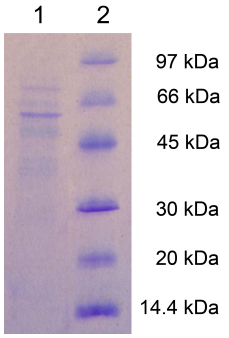

Figure 13: Purification of *Lm*SPase-D82A. Lane 1-2: 1, purified enzyme fraction; 2, LMW-standard.

Table 1: Kinetic parameters for the arsenolysis reaction of wild-type and muteins.

Reaction type	**Wild-type** k_{cat} [s^{-1}]	**F52A mutant** k_{cat} [s^{-1}]	**F52N mutant** k_{cat} [s^{-1}]	**D82A mutant** k_{cat} [s^{-1}]
Arsenolysis G1P	49	0.04	0.02	0.003
Arsenolysis Gal1P (10^{-4})	3.8	19	35	46

As seen in Table 1, the activity of the arsenolysis reaction with G1P and Gal1P was calculated to be 0.003 s^{-1} and 0.005 s^{-1}, respectively. Compared to the F52A and F52N muteins, the glucose transfer activity of the D82A mutant was about 10x lower, whereas the galactose transfer activity was slightly better.

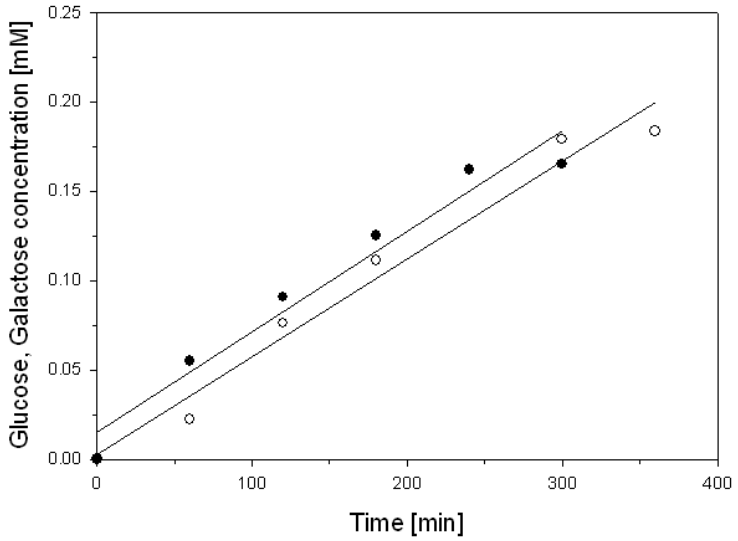

Figure 14: Time-dependent measurements of the G1P (○) and Gal1P (●) arsenolysis catalyzed by *Lm*SPase-D82A. The reported values were corrected for the blank readings. Initial-rates were determined as function of glucose or galactose release using a discontinuous assay. The enzymatic assay was performed in 50 mM MES buffer, pH 7.0 at 30°C and 550 rpm with an enzyme concentration of 0.32 mg/mL at saturating concentrations of 50 mM arsenate and 50 mM G1P or 50 mM Gal1P.

I Troubleshooting

I.1 Oligonucleotide synthesis

Oligonucleotides were ordered at VBC Biotech Services GmbH, however those primers did not anneal to the template. After ordering the oligonucleotides from Invitrogen GmbH, a PCR product was obtained.

I.2 Activity measurements from the crude cell extract

The galactose-transfer activity of the muteins was tested in synthesis direction (Gal1P + Fructose → galactopyranosyl-1,2-fructofuranoside + P_i). The rate of transfer was determined at 30°C in 70 mM MES buffer, pH 7.0 using a discontinuous assay [220 mM fructose, 180 mM Gal1P, in the presence of 0.18 mg/mL crude cell extract], in which the P_i release was determined. The crude cell extract was partially purified via ammonium sulfate precipitation before use. Thereby, the supernatant was brought to 30% ammonium sulfate and precipitated proteins were separated by ultracentrifugation. The clear supernatant was used in the assay.

Table 2: The rate of galactose-transfer was determined in a discontinuous assay, in which the P_i release [mM] was determined over time.

Time [min]	**Empty cell extract** [mM]	**F52A mutant** [mM]	**F52N mutant** [mM]	**Wild-type** [mM]
60	1.30	1.75	1.25	0.21
120	1.80	3.65	2.71	0.28
180	2.39	5.27	4.20	0.17
360	5.44	10.91	8.50	0.60

As seen in Table 2, the *Lm*SPase muteins showed a higher activity (=higher concentration of released P_i) compared to the wild-type, which led to the assumption that the muteins could use Gal1P as substrate. Thus, the muteins were purified and kinetically characterized. The release of P_i by the wild-type was lower compared to the empty *E. coli* Top10 cell extract which is quite surprising.

I.3 Purification

For purification of *Lm*SPase muteins a Phenyl Sepharose Fast Flow column (Amersham Biosciences; 2.6 x 12 cm), followed by a Fractogel EMD-DEAE column (Merck; 2.6 x 9.5 cm) were employed as described elsewhere [4]. Buffer exchange was achieved on a HiPrep 26/10 Desalting column. However, this purification procedure did not lead to a pure enzyme preparation and thus, the *Lm*SPase wild-type and muteins were subcloned from the pQE30 into the pASK-IBA7+ expression vector. The pASK-IBA7+ expression vector is equipped with a Strep-Tactin affinity tag and the *Lm*SPase wild-type and muteins were purified using a Strep-Tag column (see 1.3.2).

I.4 Detection of synthesis product by HPLC analysis

To determine the activity in synthesis direction (Gal1P + fructose → D-galactopyranosyl-1,2-fructofuranoside + P_i) a discontinuous assay [220 mM fructose, 56 mM Gal1P, in the presence of 0.4 mg/mL enzyme] was performed and the formation of D-galactopyranosyl-1,2-fructofuranoside was followed via HPLC. However, no product was detected.
HPLC analysis was performed on a LaChrom HPLC system (Merck-Hitachi) equipped with a Cation C Micro-Guard cartridge followed by an Aminex HPX-87C column (Bio-Rad) and a L-7490 RI-detector. Baseline separation was obtained when using water as eluent at a flow rate of 0.6 mL/min and a temperature of 85°C. Authentic (relevant) standards were used for peak identification, and quantification was based on peak area that was suitably calibrated with standards of known concentration.

I.5 Stability of *Lm*SPase muteins

Stability problems were encountered during the kinetic studies. When the muteins were stored at -20°C, they were active for two (F52A) and three (F52N) months, while they were only active for three (F52A) and four weeks (F52N) when stored at -4°C. An inactive mutant showed three separate bands on a SDS gel, most probably due to proteolytic cleavage.

I.6 Galactose-1-phosphate

The first studies were performed with Gal1P from Sigma-Aldrich. The second delivery of Gal1P from Sigma-Aldrich was heavily contaminated with phosphate and thus the Gal1P was further purchased from Carbosynth, which showed only minor phosphate contaminations.

References (Appendix)

[1] Eis, C. and Nidetzky, B. (1999). Characterization of trehalose phosphorylase from *Schizophyllum commune*. Biochem. J., 385-393.

[2] Saheki, S., Takeda, A., and Shimazu, T. (1985). Assay of inorganic phosphate in the mild pH range, suitable for measurement of glycogen phosphorylase activity. Anal. Biochem., 277-281.

[3] Kunst, A., Draeger, B., and Ziegenhorn, J. (1984). D-glucose. Colorimetric methods with glucose oxidase and peroxidase. Verlag Chemie, 178-185.

[4] Schwarz, A. and Nidetzky, B. (2006). Asp-196 $\rightarrow$ Ala mutant of *Leuconostoc mesenteroides* sucrose phosphorylase exhibits altered stereochemical course and kinetic mechanism of glucosyl transfer to and from phosphate. FEBS Lett., 3905-3910.